Accurate Hybrid Density Functionals with UW12 Correlation

Zack M. Williams, Timothy C. Wiles, and Frederick R. Manby*

Centre for Computational Chemistry, School of Chemistry, University of Bristol, Bristol BS8 1TS, UK

E-mail: fred.manby@bristol.ac.uk

Abstract

In previous work, we suggested a single-parameter hybrid functional containing a novel correlation contribution based on the Unsöld approximation, UW12. This model resembles the explicitly correlated part of MP2-F12 theory and can be written as an explicit formula in terms of the single-particle reduced density matrix. Here we further investigate hybrid functionals containing UW12 correlation, and in particular look at functionals with a large fractions of exact exchange to reduce the self-interaction error. We suggest two new hybrid functionals B-LYP-osUW12 and fB-LYP-osUW12. On the test sets we use, our best hybrid functional overall (B-LYP-osUW12) is of similar accuracy to the best double hybrids considered, while eliminating the need for virtual orbitals.

1 Introduction

Density functional theory (DFT)[1,2] has become the most widely used electronic structure method. While exact in principle, approximate functionals are used for all practical com-

putations. These approximations are usually relatively simple and are considered accurate enough for many chemical properties.

In (generalized) Kohn-Sham DFT,[2,3] all terms are calculated exactly except the exchange and correlation, which must be evaluated using approximate exchange correlation (xc) functionals. While there is no systematic way to improve these approximate functionals, they are often classified by their position on Jacob's Ladder.[4] Functionals higher up the ladder depend on more variables, and ascending the ladder is broadly associated with improved accuracy. Functionals on the lowest rung depend solely on the local value of the electron density, and higher rungs incorporate first and then second derivatives of the density. By the fourth rung, explicit dependence on the occupied Kohn-Sham orbitals is introduced, often through inclusion of a portion of exact Hartree-Fock exchange.[5] Finally, functionals on the fifth rung additionally depend on virtual (unoccupied) orbitals, typically including some form of non-local correlation such as Görling-Levy perturbation theory (GLPT),[6,7] or the random-phase approximation (RPA).[8]

Double-hybrid density functionals[9] constitute an important class of fifth-rung functionals, and use second-order Møller-Plesset perturbation theory (MP2) to supply the non-local correlation contribution. The MP2 correlation energy can be written

$$E_{\mathrm{c}}^{\mathrm{MP2}} = \frac{1}{2} \sum_{ijab} T_{ab}^{ij} \left\langle ab \left| r_{12}^{-1} \right| ij \right\rangle \tag{1}$$

where i, j label occupied orbitals; a, b label virtual (unoccupied) orbitals; and the double-excitation amplitudes T_{ab}^{ij} are given by

$$T_{ab}^{ij} = -\frac{\left\langle ij \left| r_{12}^{-1} \right| \overline{ab} \right\rangle}{\epsilon_a + \epsilon_b - \epsilon_i - \epsilon_j}, \tag{2}$$

with $\left|\overline{ab}\right\rangle = |ab\rangle - |ba\rangle$ and orbital energies ϵ_i.

In most double-hybrid functionals this contribution is treated non-self consistently; instead the remaining terms are used in the self-consistent-field (SCF) optimization, and a

portion of E_c^{MP2} is added as a post-SCF correction. Many more recent double hybrids use an entirely different functional for orbital optimization (usually a hybrid functional), with the double-hybrid expression only used to calculated the final energy. This method was first used for the XYG3 functional.[10,11] Orbital-optimized double hybrids have been developed,[12–14] and offer some improvement over standard double hybrids.[15,16] That said, the orbital optimization scheme is not trivial to implement, so most double hybrids have not followed this approach. More seriously, the MP2 energy expression is not bound below, so any optimization procedure must simply be locating a local minimum. The unbounded nature of the problem can be seen by considering the effect of an orbital rotation that brings an occupied and virtual orbital into degeneracy.

Double hybrid functionals offer significant improvements over standard hybrids, with improved descriptions of many molecular properties, making them the most accurate density functionals currently available.[17] However, they have a number of disadvantages not present in standard hybrid functionals. MP2 is not bound below in metals, bond-breaking situations, or as discussed above, on orbital optimization, and double hybrids inherit these deficiencies. Addition of MP2 also introduces dependence on virtual orbitals, bringing along slow basis-set convergence — a problem usually associated with wavefunction-based correlation methods. Additionally, they have increased computational scaling compared to standard hybrids, formally scaling as N^5. Finally, use of non-stationary orbitals also leads to problems for spin-unrestricted calculations and calculation of first-order properties.[18]

Despite the large number of exchange-correlation functionals now available, there are still multiple problems encountered when using these approximations. One of the most significant sources of error is the self-interaction error (SIE). For a system with one electron or less, the electron-electron interaction energy should be zero. Therefore, the sum of the Coulomb and exchange-correlation energies should vanish

$$J[\rho] + E_{xc}[\rho] = 0 \tag{3}$$

for all electron densities ρ satisfying $\int \rho \leq 1$. However, approximate exchange-correlation functionals typically break this condition, and the resulting energy error defines the one-electron SIE. This error is also present in many-electron systems, though it is difficult to distinguish from the many-electron SIE effects.[19]

Delocalization error is a related concept, and is defined using the error in approximate functionals when describing systems with fractional charge.[20] The exact ground-state energy of a system varies in a piecewise-linear way with electron number, such that[21]

$$E(N+\delta) = (1-\delta)E(N) + \delta E(N+1) \tag{4}$$

for integer N and $0 \leq \delta \leq 1$. Note that this equation results in derivative discontinuities at integer electron numbers due to the piecewise linear behavior.

Approximate density functionals do not satisfy this condition, underestimating the energy at fractional values and as such suffer from 'delocalization error'. This term is used since the phenomena is most readily observed in systems where electrons become delocalized, resulting in fractionally charged fragments.

Despite efforts to eliminate self-interaction and delocalization errors, they are still one of the major limitations of current density functionals.[22] However, double-hybrid functionals have achieved some success at reducing these errors.[11,17] In this work, we aim to achieve similar success using hybrid functionals incorporating our UW12 correlation model, thereby avoiding the drawbacks of MP2-based double hybrids.

2 Theory

We previously defined the UW12 correlation energy as[23]

$$E_c^{\mathrm{UW12}} = \frac{1}{2} \sum_{ijab} \left\langle ij \left| w_{12} \right| \overline{ab} \right\rangle \left\langle ab \left| r_{12}^{-1} \right| ij \right\rangle \tag{5}$$

where w_{12} is a two-particle 'geminal' operator. The expression resembles MP2 (equations (1) and (2)) with the double excitation amplitudes replaced by

$$T_{ab}^{ij} = \left\langle ij \left| w_{12} \right| \overline{ab} \right\rangle , \tag{6}$$

making the UW12 energy independent of the orbital energies.

Removing the energy denominator makes it possible to eliminate the sum over virtuals, in exactly the way that Unsöld did in the constant-denominator approximation. As a result the energy can be written in a form which depends only on the occupied Kohn-Sham spin-orbitals $\{\phi_i\}$:

$$E_{\mathrm{c}}^{\mathrm{UW12}} = E_{\mathrm{c,2el}}^{\mathrm{UW12}} + E_{\mathrm{c,3el}}^{\mathrm{UW12}} + E_{\mathrm{c,4el}}^{\mathrm{UW12}} \tag{7}$$

where the two-, three-, and four-electron terms are given by

$$E_{\mathrm{c,2el}}^{\mathrm{UW12}} = \frac{1}{2} \sum_{ij} \left\langle \overline{ij} \left| w_{12} r_{12}^{-1} \right| ij \right\rangle \tag{8}$$

$$E_{\mathrm{c,3el}}^{\mathrm{UW12}} = -\sum_{ijk} \left\langle \overline{ij}k \left| w_{12} r_{23}^{-1} \right| kji \right\rangle \tag{9}$$

$$E_{\mathrm{c,4el}}^{\mathrm{UW12}} = \frac{1}{2} \sum_{ijkl} \left\langle ij \left| w_{12} \right| \overline{kl} \right\rangle \left\langle kl \left| r_{12}^{-1} \right| ij \right\rangle . \tag{10}$$

Since this UW12 energy depends only on the occupied orbitals, the basis set convergence is faster than for the MP2 energy expression. Orbital optimization also becomes trivial as the energy is now a specific, simple formula in terms of the one-particle reduced density matrix, and there is no energy denominator that can lead to divergence. The geminal operator w_{12} is chosen to be a function of the inter-electronic distance r_{12} and the total spin of the two electrons $s_{12} = \delta_{\sigma_1\sigma_2}$. We use a Slater-type geminal commonly used in explicitly correlated methods[24–26]

$$w_{12} = -\frac{1}{2(s_{12}+1)} r_c \exp\left[-\frac{r_{12}}{r_c} \right] \tag{11}$$

with a single length-scale parameter r_c.

Using this approximation, we created a new functional with parameters based on BH&HLYP and B2-PLYP; the first hybrid and double hybrid functionals introduced.[5,9] This functional, XCH-BLYP-UW12

$$E_{\mathrm{xc}}^{\text{XCH-BLYP-UW12}} = \frac{1}{2}E_{\mathrm{x}}^{\mathrm{B88}} + \frac{1}{2}E_{\mathrm{x}}^{\mathrm{HF}} + \frac{3}{4}E_{\mathrm{c}}^{\mathrm{LYP}} + \frac{1}{4}E_{\mathrm{c}}^{\mathrm{UW12},r_c}, \tag{12}$$

was shown to be accurate for atomization energies and reaction barrier heights, despite containing only a single parameter, empirically set to $r_c = 1.7\,a_0$. The functional also contains a larger fraction of exact exchange ($a_{\mathrm{x}}^{\mathrm{HF}} = 0.5$) than standard hybrid functionals such as B3LYP ($a_{\mathrm{x}}^{\mathrm{HF}} = 0.2$) and PBE0 ($a_{\mathrm{x}}^{\mathrm{HF}} = 0.25$).[27–29]

More recent double hybrid functionals such as DSD-BLYP, and XYG3 contain even larger fractions of exact exchange, around 0.75 and 0.80 respectively[30].[10,31,32] This gives other advantages over global single-hybrids by reducing the self-interaction error in the functional. Here we investigate a UW12 functional containing a large fraction of exact exchange to minimize the amount of self-interaction; while studying the effect on the overall accuracy of the functional.

We limit ourselves to considering only GGA density functionals for the local exchange–correlation, namely Becke's 1988 (B88) exchange functional and Lee-Yang-Parr (LYP) correlation.[33,34] In principle, any similar semi-local exchange and correlation functionals could be used for the density functional part of the hybrids,[35] and could be optimized alongside other parameters. We had previously looked at PBE based functionals for which results were similar. We also consider only global hybrid functionals with fixed fractions of exact exchange and UW12 correlation.

Many modern double-hybrid functionals use meta-GGA exchange-correlation terms or range-separated exchange, such as the recent ωB97M(2) functional.[36] This 14-parameter functional uses a combinatorial optimization procedure to expand the exchange-correlation functionals into a Becke-Handy power series.[37,38] However, our intent here is to evaluate

functionals containing a minimal number of parameters to assess the accuracy of UW12 as a correlation approximation combined with standard density functional components. More extensive parameterization could be applied to UW12 functionals in the future. In order to assess the accuracy of our functional, we compare to similarly constructed double-hybrid functionals (BLYP based global hybrids).

2.1 Frozen Core Approximation

Previously, we calculated the UW12 correlation energy for all electrons in the system. However, most correlation methods employ the frozen-core approximation where only the valence electrons are correlated. For double hybrids, the frozen-core approximation has a minimal effect on results, assuming that parameters are re-optimized for the frozen-core case.[31] Our incentive here is to avoid having to compromise the length-scale parameter r_c between valence and core electrons; for this reason we use the frozen-core UW12 approximation unless otherwise noted.

For UW12, the frozen-core energy is defined by equation (5) with occupied orbitals i, j summed only over the active (valence) orbitals. However, in order to remove the virtual orbitals, we use the identity

$$\sum_{ab} \left|\overline{ab}\right\rangle \langle ab| = \sum_{pq} \left|\overline{pq}\right\rangle \langle pq| + \sum_{kl} \left|\overline{kl}\right\rangle \langle kl| - \sum_{kp} \left|\overline{kp}\right\rangle \langle kp| - \sum_{kp} \left|\overline{pk}\right\rangle \langle pk| \,, \qquad (13)$$

for a complete space of virtual orbitals a, b, occupied orbitals k, l, and the full set of orbitals p, q; the summations involving occupied orbitals include both core and valence orbitals. The resulting two-, three-, and four-electron terms, previously shown in equations (8) to (10),

become:

$$E_{\mathrm{c,2el}}^{\mathrm{UW12}} = \frac{1}{2} \sum_{i,j \in \mathrm{val.}} \left\langle \overline{ij} \left| w_{12} r_{12}^{-1} \right| ij \right\rangle \tag{14}$$

$$E_{\mathrm{c,3el}}^{\mathrm{UW12}} = - \sum_{\substack{i,j \in \mathrm{val.} \\ k \in \mathrm{occ.}}} \left\langle \overline{ij}k \left| w_{12} r_{23}^{-1} \right| kji \right\rangle \tag{15}$$

$$E_{\mathrm{c,4el}}^{\mathrm{UW12}} = \frac{1}{2} \sum_{\substack{i,j \in \mathrm{val.} \\ k,l \in \mathrm{occ.}}} \left\langle ij \left| w_{12} \right| \overline{kl} \right\rangle \left\langle kl \left| r_{12}^{-1} \right| ij \right\rangle . \tag{16}$$

2.2 Spin-Component Scaling

Spin-component scaling (SCS) scales the opposite and same spin contributions to the correlation by different values. Following the introduction of spin-component scaled SCS-MP2,[39] this approach has been applied to various correlation methods.[40] Early double hybrid functionals such as B2-PLYP use the standard MP2 expression.[9] More recent double hybrids utilize spin-scaling, notably the DSD-DFT-type double hybrids.[31,32,41] These functionals offer some additional improvement over basic double hybrids.[17]

Spin scaling can alternatively be applied such that the same-spin contribution is neglected altogether — this is known as scaled-opposite-spin (SOS) or opposite-spin only.[42] This approach is often used with double hybrids to reduce the overall scaling of the method,[32,43–45] and it has been shown that this can be done without significant loss of accuracy. In addition, most RPA-based methods in DFT are opposite-spin only.[8,40,46] In this work we include only the opposite spin ($s_{12} = 0$) component of UW12. For this model, the amplitudes are now given by

$$T_{ab}^{ij} = \langle ij \left| w_{12} \right| ab \rangle \tag{17}$$

with the geminal function

$$w_{12} = \begin{cases} -\frac{1}{2} r_c \exp\left[-\frac{r_{12}}{r_c} \right] & s_{12} = 0 \\ 0 & s_{12} = 1 \end{cases} \tag{18}$$

Previously, we used the constraints that $a_{\mathrm{c}}^{\mathrm{LYP}} + a_{\mathrm{c}}^{\mathrm{UW12}} = 1$ and $a_{\mathrm{c}}^{\mathrm{UW12}} = \left(a_{\mathrm{x}}^{\mathrm{HF}}\right)^2$; here we relax these restraints and allow the opposite spin UW12 factor to be an adjustable parameter, $a_{\mathrm{c}}^{\mathrm{UW12,os}}$.

2.3 Empirical Dispersion

Dispersion corrections in DFT are important for the description of non-bonding (long-range) interactions. In particular, most standard density functional approximations do not provide an adequate description of non-local dispersion forces.[47,48] Performance of double-hybrids has been shown to improve by using an empirical dispersion term.[32,49]

In this paper, we consider the effect of a DFT-D3(BJ) dispersion correction with Becke-Johnson damping.[50–52] In this method, the dispersion correction is given by

$$E_{\mathrm{disp}}^{\mathrm{D3(BJ)}} = -\frac{1}{2} \sum_{A \neq B} \sum_{n=6,8} s_n \frac{C_{(n)}^{AB}}{R_{AB}^n} f_{\mathrm{damp}}^{(n)}(R_{AB}) \tag{19}$$

for interatomic distances R_{AB}, scale factors s_n, dispersion coefficients $C_{(n)}^{AB}$, and Becke-Johnson damping function $f_{\mathrm{damp}}^{(n)}$ given by

$$f_{\mathrm{damp}}^{(n)}(R_{AB}) = \frac{R_{AB}^n}{R_{AB}^n + (a_1 R_{AB}^0 + a_2)^n}, \tag{20}$$

for parameters a_1, a_2, and $R_{AB}^0 = \sqrt{C_8^{AB}/C_6^{AB}}$. The more recent D4 dispersion model uses a similar form with an updated scheme for computing C_6 coefficients[53].[54]

Formally, the s_6 parameter should be equal to one. However, for double hybrids it must be optimised since some long-range behaviour is captured by the MP2 term. This is due to the coulomb operator in the two-electron integrals which results in a leading order correction $\sim 1/R^3$, resulting in the correct $\sim 1/R^6$ behaviour for the overall energy.[55–57] For the UW12 approximation, this correct long-range behaviour is not replicated, since the Coulomb operator is replaced by the UW12 geminal operator in one of the integrals. For

the case of a Slater-type geminal, the geminal operator acts over a much shorter range than the Coulomb term, making UW12 a short-range theory.

2.4 UW12 Hybrid Functionals

We define a new functional form: B-LYP-osUW12(-D3BJ)

$$E_{\mathrm{xc}}^{\text{B-LYP-osUW12}} = (1 - a_{\mathrm{x}}^{\mathrm{HF}})E_{\mathrm{x}}^{\mathrm{B88}} + a_{\mathrm{x}}E_{\mathrm{x}}^{\mathrm{HF}} + a_{\mathrm{c}}^{\mathrm{LYP}}E_{\mathrm{c}}^{\mathrm{LYP}} + a_{\mathrm{c},s=0}^{\mathrm{UW12}}E_{\mathrm{c},s=0}^{\mathrm{UW12},r_c}\,(+E_{\mathrm{D3BJ}}) \qquad (21)$$

This functional contains opposite spin UW12 only and resembles the DOD-BLYP double-hybrid,[32] with UW12 correlation instead of MP2. This new functional contains four adjustable (non-dispersion) parameters, a similar number to many double-hybrid functionals.

2.5 Orbital Optimization

Unlike MP2, the UW12 energy is an explicit formula in terms of the one-particle reduced density matrix. As a result, the orbitals in a UW12 calculation may be optimized fully self-consistently, and the Fock matrix can be evaluated (using density-fitting) in a computational time which scales formally with system size as N^4.[23] This is the same formal scaling as the HF exchange energy.

In this work, orbital optimization was not performed during fitting. Instead each component in the energy expression was evaluated for fixed B3LYP orbitals.[58] The XYG3 type of double hybrid functionals are calculated in this way,[10,11] as well as ωB97M(2) among others.[36] Fitting the parameters in this way simplifies the procedure, but has the disadvantage that the resulting functional may not be as accurate as if the parameters were adjusted in conjunction with the orbital-optimization. In future we hope to include orbital-optimization in the parameterization, a standard procedure for many double-hybrid functionals.[59] Once the functional parameters have been optimized; the self-consistent results may be calculated. We later show that the energy differences observed by changing to the minimized orbitals

has only a small effect on results in most cases.

3 Computational Details

The test sets used in this paper are subsets of the GMTKN30 and GMTKN55 databases.[17,43] The test sets used cover a range of molecular properties, and all geometries and reference values were taken from the Mulliken Center website.[60] The complete list of test sets included in this paper is given in the supporting information.

For comparison between correlation energies, molecules from the G2/97 test set were used, which were optimized at the MP2(full)/6-31G* level.[61–63 64] GMTKN30 double-hybrid and SIE4x4 coupled-cluster calculations were performed in Molpro.[65–68] Density-fitted coupled-cluster calculations on the G2/97 test set were performed in Psi4.[69,70] HF, MP2 and FCI potential energy scans of H_2 were performed in PySCF.[71,72] All other calculations were performed in Entos Qcore unless otherwise stated.[73,74] Fractional calculations on atomic ions used the aug-cc-pV(Q+d)Z basis set,,[75–79] calculations for the G21EA,[80] IL16 and AHB21[81] use the aug-cc-pVQZ basis set. All other calculations use the Def2-QZVP basis set along with the associated auxiliary basis sets for density fitting.[82–84] Quadruple-zeta basis sets are used to allow direct comparison with double hybrid functionals. Grid based calculations use the Neese fixed prune quadrature grids[85];[86] in addition grids in Entos Qcore use a modified Becke partitioning for construction of the quadrature grid.[87]

All double-hybrid and UW12 functionals use the frozen-core approximation when correlating electrons, except for XCH-BLYP-UW12 which was not optimized using the frozen-core approximation.

4 Results and Discussion

The aims of this section are: to show that the UW12 method can be used to approximate accurate correlation energies (section 4.1); to optimize UW12 based functionals to achieve

double-hybrid levels of accuracy (section 4.2); to study self-interaction and delocalization errors of the new functionals (section 4.3).

In order to assess the accuracy of the functionals, we compare to a number of established hybrid and double-hybrid functionals, namely: B2-PLYP,[9] B3LYP,[27,28] DOD-BLYP,[88] DSD-BLYP,[89] XYGJ-OS.[90] We study the accuracy of these both with and without dispersion. In addition we also compare to three MP2 methods: standard MP2,[91] SCS-MP2,[39] and SOS-MP2.[42]

4.1 Correlation Energy

A major aim in using the UW12 approximation is to be able to reproduce accurate correlation energies of other wavefunction based methods. In this section we compare UW12 correlation energies to those of MP2 and CCSD(T). For a direct comparison the UW12 correlation energies are evaluated non-self-consistently using HF orbitals, with the energy calculated using the 'MP2-like' formula given in equation (5) which includes the virtual orbitals. While this formula is not the typical method we use to calculate the UW12 energy, it is useful for direct comparison with MP2 and coupled cluster.

Correlation energies were calculated for all closed-shell molecules in the G2/97 test set. Figure 1 shows the distribution of errors in the correlation energies for (unscaled) correlation methods MP2 and UW12, as well as the opposite spin only versions. These results cover closed-shell singlet correlation energies for molecules in the G2/97 test set using CCSD(T) values as a reference. The range parameter used in this plot is $r_c = 2.6\,a_0$ (see section 4.2), and we note that this value has not been optimized specifically for this data.

From this plot it can be seen that UW12 results in the overall lowest error in correlation energies compared with CCSD(T). The distribution of errors is significantly smaller than for MP2 or osMP2. Neglecting the same-spin contribution results in a small increase in errors, though this appears to be less pronounced for osUW12 than for osMP2, which has the largest error and distribution of errors. The opposite spin only UW12 correlation still

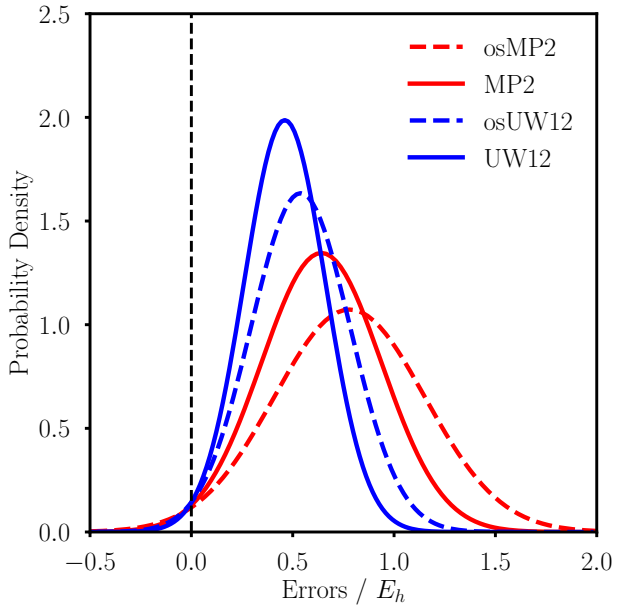

Figure 1: Plot showing the distribution of errors in the correlation energies for closed shell G2-97 molecules calculated for each method with CCSD(T) as a reference. All values were calculated using the Def2-QZVP basis set with density fitting. UW12 correlation energies were calculated using the Slater-type geminal function in equation (11) with range parameter $r_c = 2.6\, a_0$. The prefix 'os' refers to (unscaled) opposite spin only values.

has a smaller mean error than MP2. This demonstrates that it is possible to use UW12 to calculate correlation energies to a similar accuracy as MP2.

As an additional test of the UW12 correlation energy, we look at the dissociation of a hydrogen molecule, for this we consider the two cases where the wavefunction is restricted and unrestricted. Figure 2 shows the energy of the H_2 molecule as a function of bond length with correlation energies calculated using both MP2 and UW12. In the restricted case, at short bond lengths MP2 is shown to give the correct behaviour. However, for bond distances greater than around $5\, a_0$, the MP2 energy behaves in a none physical way and starts to decrease. UW12 does not replicate this behaviour and continues to behave in a physically correct manner at large distances.

In the unrestricted case MP2 is close to the exact solution around the equilibrium bond length. At around $2.5\, a_0$, the MP2 energy diverges from the exact solution with a visible discontinuity in the gradient of the curve. The error in the UW12 energy compared to the

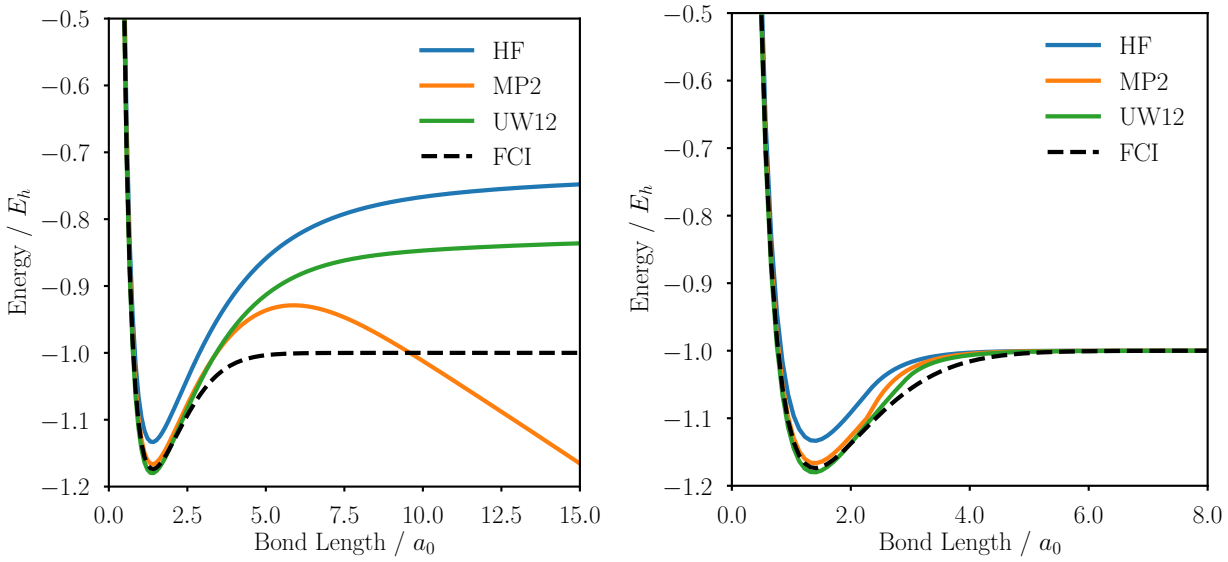

(a) Restricted

(b) Unrestricted

Figure 2: Plots showing the potential energy curves for a molecule of hydrogen calculated using HF, MP2, UW12, and FCI, for both restricted and unrestricted cases. All energies were calculated using the Def2-QZVP basis set. UW12 denotes the total energy of HF with UW12, calculated using $r_c = 2.6\,a_0$.

exact solution also increases in this intermediate region. However, not to the same extent as MP2 and follows a continuous slope.

To study this further, we plot the error in the energy for each of these cases compared to FCI. Figure 3 shows the error in the HF, MP2, and UW12 energies. This plot clearly shows the derivative discontinuity in the MP2 energy at the Coulson-Fischer point around $2.3\,a_0$. The UW12 energy varies smoothly in this region, because of the self-consistent optimization. The maximum error in HF occurs around $2.4\,a_0$, near the Coulson-Fischer point. UW12 is just another meanfield method, so it too has a Coulson-Fischer point, occuring around $2.9\,a_0$. Similarly this is close to the maximum error in the energy, however the error varies smoothly in this region.

Overall, this illustrates that UW12 does not suffer an unphysical breakdown for the simplest stretched bond, and the overall correlation energy does not undergo the same unphysical derivative discontinuity as the MP2 energy. However, adding UW12 to HF does not remove the Coulson-Fischer point, instead shifting it to a longer bond length.

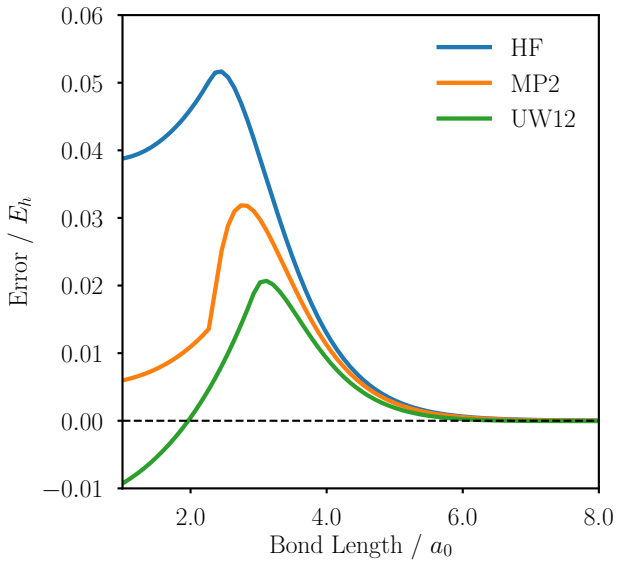

Figure 3: Plot showing error in the energy of HF, MP2, and UW12 compared to FCI as a function of bond length.. Here, we define the UW12 energy as the fully-self-consistent HF+UW12 energy, with UW12 calculated using range parameter $r_c = 2.6\,a_0$. All values were calculated using the Def2-QZVP basis set.

4.2 Functional optimization

In this section we look at optimizing the parameters in B-LYP-osUW12. We are looking to create a functional with a high fraction of exact exchange, $a_{\mathrm{x}}^{\mathrm{HF}} \sim 0.75$, since this amount has been shown to minimize the delocalization error. Therefore, we consider two cases; the fixed case where we set $a_x^{\mathrm{HF}} = 0.75$ and optimize the remaining parameters, and the free case where we optimize all parameters. The resulting functionals are named fB-LYP-osUW12 and B-LYP-osUW12 respectively. We wish to analyze the effect of fixing the amount of exact exchange compared with fitting the parameter. To study the effect of dispersion on results, we also optimize B-LYP-osUW12 both with and without a D3BJ dispersion correction.

To fit the parameters for a given number of test sets, we sum the root mean square errors (RMSEs) for each set, weighted by the ratio of the number of relative energies N_i in the test set and the root mean square of the absolute reference energies of the test sets ΔE_{RMS}. The result is then scaled by the ratio of the mean ΔE_{RMS} value and the total number of relative

energies for all test sets included:

$$\Delta = \frac{\overline{\Delta E}_{\mathrm{RMS}}}{\sum_i N_i} \sum_j \frac{N_j}{\Delta E_{\mathrm{RMS},j}} \times \mathrm{RMSE}_j \tag{22}$$

This procedure is somewhat similar to the WTMAD-2 proposed in Ref. 17, except using root mean square values instead of mean absolute values. We elect to use RMSEs to optimise the functionals rather than mean absolute errors (MAEs) as we would like to use this to eliminate outliers, to which the RMSE is more sensitive. We will later use the MAE to assess the accuracy of these functionals once optimized.

To evaluate the UW12 integrals, we expand the geminal function as a series of Gaussians and optimize the coefficients for a given set of exponents using the procedure outlined in Ref. 23. In order to optimize the functional, we calculate the unscaled contribution of each component of the geminal expansion separately for each system.[92] During fitting, the optimal coefficients for a given range parameter r_c are calculated at each step, and the total UW12 energy for each system is calculated as the sum of the (pre-calculated) energy components weighted by the corresponding coefficient.

We apply the fitting procedure to the functionals, to minimize the value of Δ, with the resulting optimized parameters shown in table 1. This table also shows the parameters used

Table 1: Table of parameters for the UW12 functionals. Values in bold are optimized.

	$a_{\mathrm{x}}^{\mathrm{HF}}$	$a_{\mathrm{x}}^{\mathrm{B88}}$	$a_{\mathrm{c}}^{\mathrm{LYP}}$	$a_{\mathrm{c}}^{\mathrm{osUW12}}$	$a_{\mathrm{c}}^{\mathrm{ssUW12}}$	r_c/a_0
B-LYP-osUW12	**0.57**	**0.43**	**0.43**	**0.43**	0.00	**2.6**
fB-LYP-osUW12	0.75	0.25	**0.12**	**0.76**	0.00	**2.0**
XCH-BLYP-UW12	0.50	0.50	0.75	0.25	0.25	**1.7**
B-LYP-osUW12-D3BJ	**0.51**	**0.49**	**0.40**	**0.52**	0.00	**1.7**

in the XCH-BLYP-UW12 functional, the B-LYP-osUW12-D3BJ functional shown contains only a leading order $1/R^6$ D3BJ term with damping parameters $a_1 = 0.0$, $a_2 = 5.45$. From this it can be seen that the new functionals contain a much larger fraction of UW12 correlation than the previous functional, combined with a much lower fraction of LYP correlation.

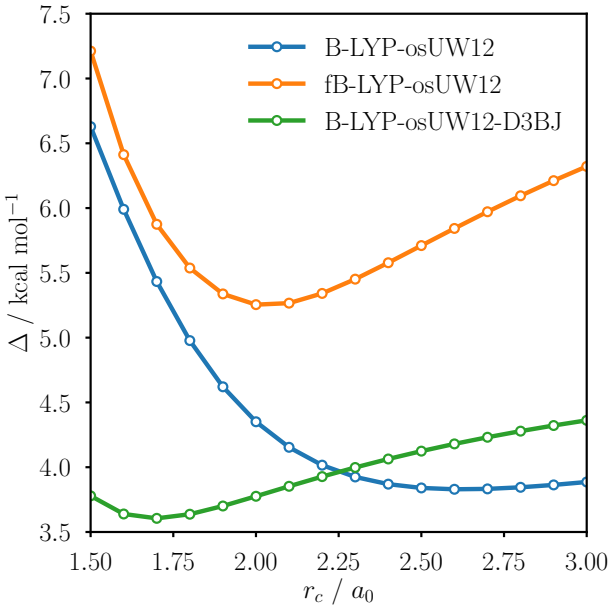

Figure 4: Plot showing the value of the error measure Δ for the considered test sets as a function of UW12 range parameter r_c for B-LYP-osUW12, fB-LYP-osUW12 and B-LYP-osUW12-D3BJ. The remaining parameters for each functional are re-optimized at each point with a fixed D3BJ correction for B-LYP-osUW12-D3BJ.

The ratio of these two correlations is further increased for a higher fraction of exact exchange, with a much lower optimal amount of LYP correlation for fB-LYP-osUW12 compared with B-LYP-osUW12. For both B-LYP-osUW12 and fB-LYP-osUW12, the optimal range parameter r_c is greater than the value for XCH-BLYP-UW12. However, re-optimization of B-LYP-osUW12 with dispersion reduces the range parameter to the same value as that of XCH-BLYP-UW12. To illustrate this, figure 4 shows the error measure Δ as a function of r_c for the three functionals. At each point on this plot the remaining parameters are refitted with a fixed D3BJ correction for B-LYP-osUW12-D3BJ. The fixed fB-LYP-osUW12 functional has a clear minimum at around $r_c = 2.0\,a_0$, with the error rising sharply for greater r_c values. While for B-LYP-osUW12 there is no significant increase in error for $r_c > 2.6\,a_0$, the optimum value. The minimum value of Δ for fB-LYP-osUW12 is also significantly greater than for B-LYP-osUW12, with B-LYP-osUW12 having a lower error than the optimal fB-LYP-osUW12 for all $r_c > 1.7\,a_0$. For B-LYP-osUW12-D3BJ the minimum value of Δ is further reduced, with a smaller value of r_c being optimal. Increasing the value of r_c increases

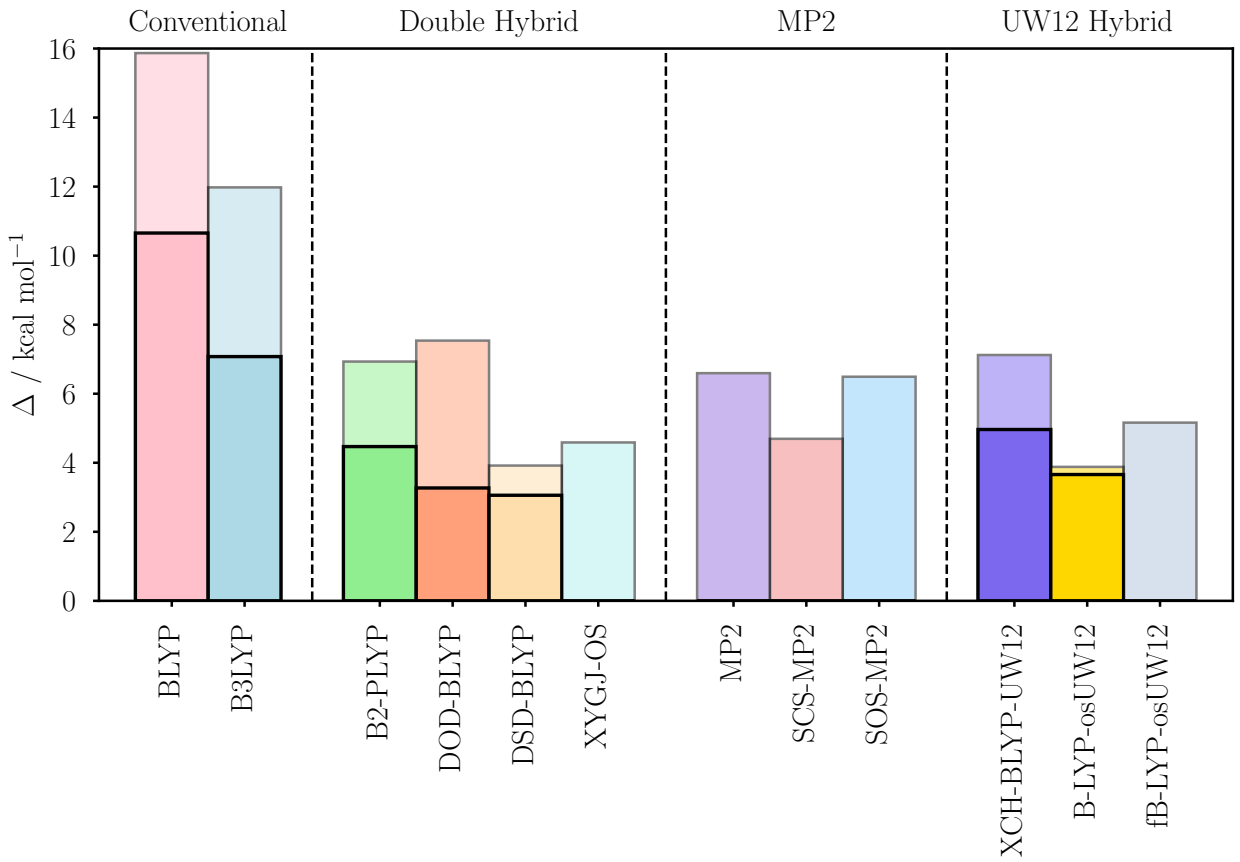

Figure 5: Plot showing the value of the error measure Δ for a number of functionals including the new UW12 hybrid functionals. Dispersion corrected functionals are shown in bold, while non-dispersion functionals are translucent. Methods without a bold bar have no dispersion-corrected counterpart. UW12 functionals shown are fully self-consistent. The dispersion-corrected XCH-BLYP-UW12-D3BJ uses the B2-PYLP D3BJ correction which we had previously done in Ref. 23. All results use the Def2-QZVP basis set.

Δ, with the dispersion-free version having a lower value of Δ for $r_c > 2.25\,a_0$.

Increasing the value of r_c increases the range of the UW12 correlation. Hence the greater values of r_c for non-dispersion corrected functionals are better since they help to capture some long range behaviour. With a dispersion correction, this long-range behaviour is accounted for so a lower value of r_c is more accurate.

Figure 5 shows the optimal Δ values for the newly optimized functionals as well as for a number of other functionals both with and without dispersion. Notice that B-LYP-osUW12 has the smallest Δ value of all the non-dispersion corrected functionals considered ($\Delta_{\text{B-LYP-osUW12}} = 3.88\,\text{kcal mol}^{-1}$), DSD-BLYP has the next lowest value with $\Delta_{\text{DSD-BLYP}} =$

$3.92\,\mathrm{kcal\,mol^{-1}}$. Also of note is the result for the XYGJ-OS functional ($\Delta_{\text{XYGJ-OS}} = 4.59\,\mathrm{kcal\,mol^{-1}}$), which contains only opposite spin MP2, a high fraction of exact exchange ($a_{\text{x}}^{\text{HF}} = 0.7731$), and uses B3LYP orbitals with four parameters. For the fixed-exchange hybrid fB-LYP-osUW12, the error is greater than the fully optimized B-LYP-osUW12 ($\Delta_{\text{fB-LYP-osUW12}} = 5.26\,\mathrm{kcal\,mol^{-1}}$). However it still performs better than the B2-PLYP and DOD-BLYP functionals as well the previous UW12 functional XCH-BLYP-UW12.

Looking at the dispersion-corrected functionals; a small improvement is seen for B-LYP-osUW12-D3BJ compared to B-LYP-osUW12 ($\Delta_{\text{B-LYP-osUW12}} = 3.66\,\mathrm{kcal\,mol^{-1}}$), while for DSD-BLYP(D3BJ), the value of Δ is greatly reduced to less than that of B-LYP-osUW12-D3BJ ($\Delta_{\text{DSD-BLYP(D3BJ)}} = 3.06\,\mathrm{kcal\,mol^{-1}}$). DOD-BLYP(D3BJ) also has a value of Δ smaller than B-LYP-osUW12. B-LYP-osUW12-D3BJ continues to perform better than B2-PLYP(D3BJ). However B2-PLYP(D3BJ) has a smaller value of Δ than XCH-BLYP-UW12-D3BJ, the two of which previously showed similar errors without dispersion. However, we note that they both use the same dispersion correction which was optimized for B2-PLYP and not XCH-BLYP-UW12.

These result show that we are able to create UW12 hybrid functionals with double hybrid accuracy with our new functional B-LYP-osUW12 outperforming DSD-BLYP without dispersion. Addition of dispersion increases the accuracy of of B-LYP-osUW12 but not as much as it does for the double hybrids.

While the results for B-LYP-osUW12 are shown to be of high quality and were achieved with a relatively small number of parameters, these parameters were fitted for this database. To properly study the accuracy, we therefore use our optimized functionals on a subset of the much larger GMTKN55 database.[17] This database contains 55 test sets of which 37 are new or extensions of previous GMTKN30 test sets. The subset we have used contains 44 of the GMTKN55 test sets of which 30 are new or extended.

For this analysis, we use the weighted mean absolute error (MAE), which is calculated in an analogous way to equation (22) using MAE instead of RMSE. This is done since studies

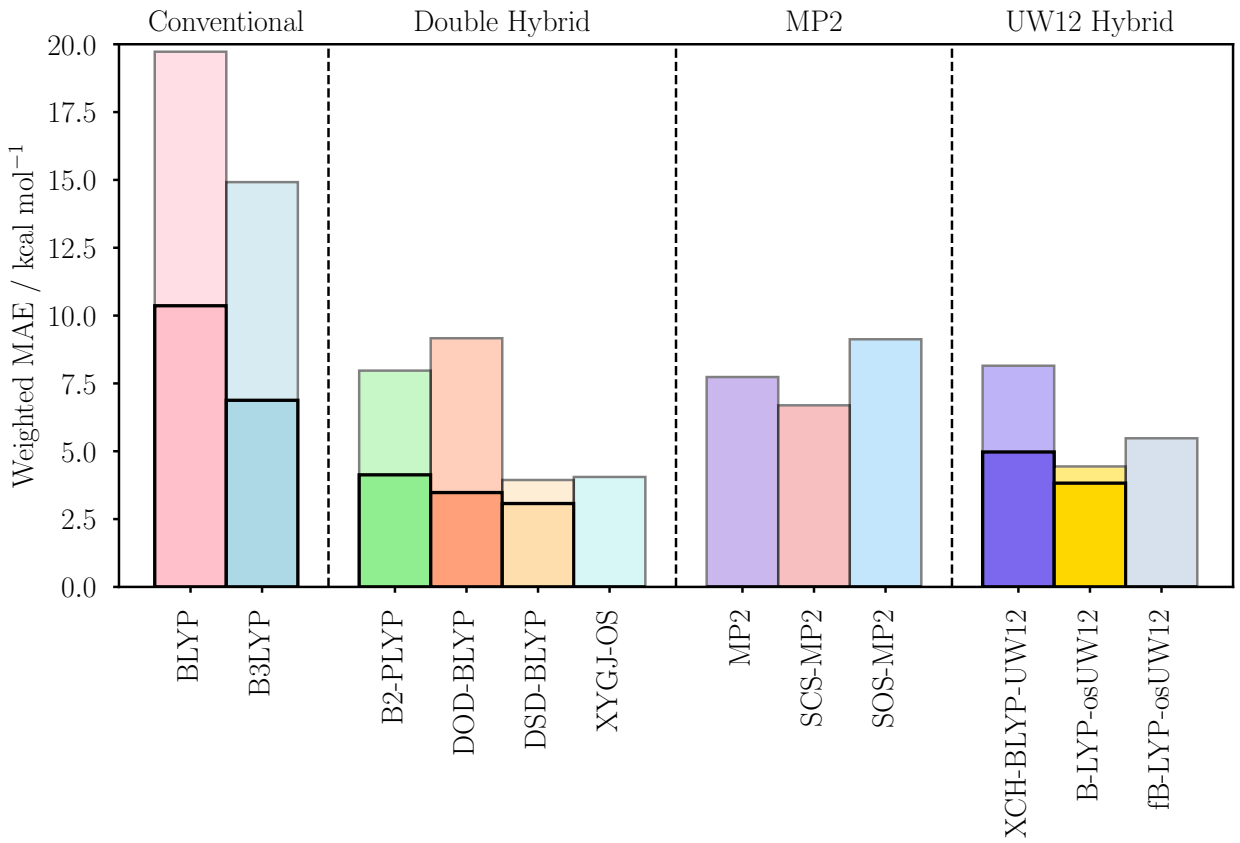

Figure 6: Plot showing the value of the weighted mean absolute error across 44 data sets of the GMTKN55 database for a number of functionals including the new UW12 functionals calculated self-consistently. Results are calculated using the Def2-QZVP basis set on 41 of the 44 test, while the anion test sets G21EA,[80] IL16 and AHB21[81] use the aug-cc-pVQZ basis set. Dispersion corrected functionals are shown in bold, while uncorrected functionals are translucent.

focussed on the full GMTKN55 database use the WTMAD-2 metric to assess functionals which is based on MAE. Figure 6 shows the weighted mean absolute error values for each of the functionals both with and without dispersion. The general trend in these results is somewhat similar to the trend in Δ values for the GMTKN30 subset. For the dispersion uncorrected functionals, this plot shows that B-LYP-osUW12 continues to perform better than the XCH-BLYP-osUW12 and fB-LYP-osUW12 functionals, as well as the B2-PLYP and DOD-BLYP functionals. However, both DSD-BLYP and XYGJ-OS display a smaller overall error than B-LYP-osUW12 ($\mathrm{wMAE_{DSD\text{-}BLYP}} = 3.94\,\mathrm{kcal\,mol^{-1}}$, $\mathrm{wMAE_{XYGJ\text{-}OS}} = 4.05\,\mathrm{kcal\,mol^{-1}}$ compared to $\mathrm{wMAE_{B\text{-}LYP\text{-}osUW12}} = 4.44\,\mathrm{kcal\,mol^{-1}}$).

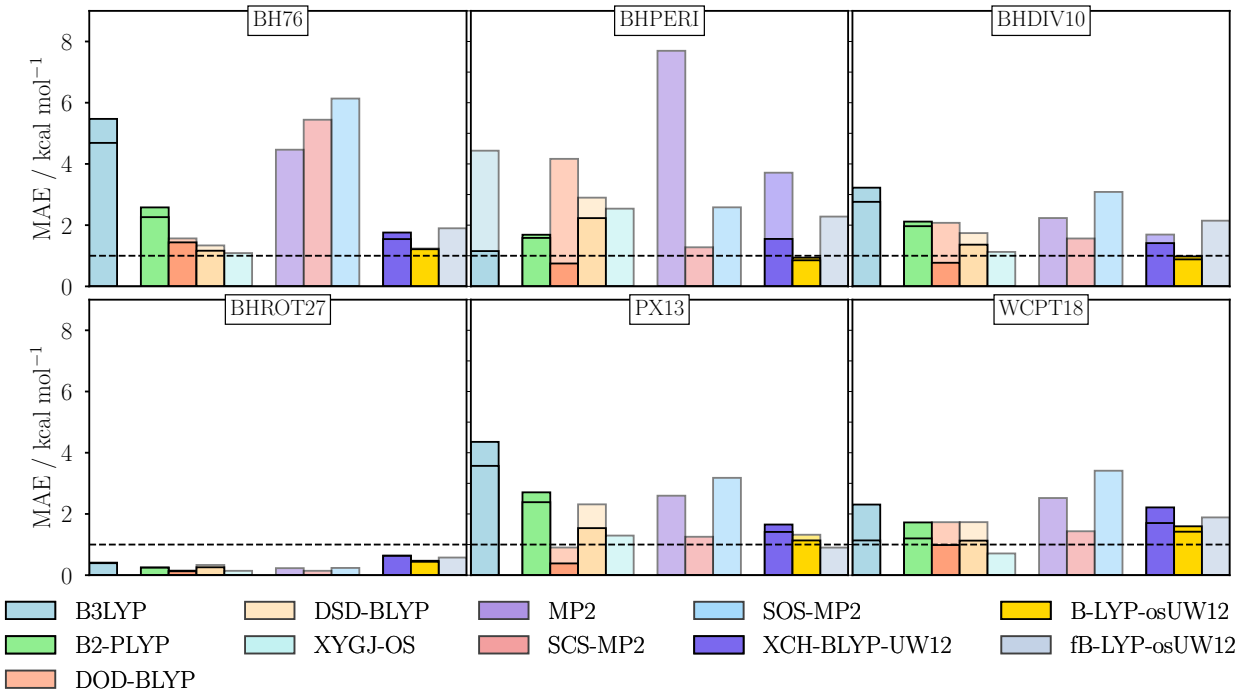

Figure 7: Mean absolute errors (MAE) for the barrier heights test sets BH76,[93,94] BHPERI,[95–98] BHDIV10,[17] BHROT27,[17] PX13,[99] and WCPT18.[100] Chemical accuracy (1 kcal mol^{-1}) is indicated by the dotted lines. Dispersion corrected functionals are shown in bold, while uncorrected functionals are translucent.

For the dispersion corrected functionals, both DSD-BLYP(D3BJ) and DOD-BLYP(D3BJ) result in lower errors than B-LYP-osUW12-D3BJ (wMAE$_{\text{DSD-BLYP(D3BJ)}}$ = 3.07 kcal mol^{-1}, wMAE$_{\text{DOD-BLYP(D3BJ)}}$ = 3.48 kcal mol^{-1} compared to wMAE$_{\text{B-LYP-osUW12-D3BJ}}$ = 3.82 kcal mol^{-1}). However B-LYP-osUW12-D3BJ continues to perform better than B2-PLYP(D3BJ), while the error for XCH-BLYP-UW12-D3BJ is shown to be greater than that of B2-PYLP(D3BJ). The overall improvement in results for B-LYP-osUW12 when dispersion is included is not as large as the improvement for DSD-BLYP.

Reaction barrier heights. Figure 7 shows the results for the barrier heights test sets considered. Of these test sets, both BH76 and BHPERI are in the training set, while the remaining four are new for GMTKN55. These sets cover a range of different barrier heights. The BH76 barrier height test set covers hydrogen transfer and non-hydrogen transfer barrier heights and is a superset of the earlier HTBH38 and NHTBH38 test sets,[93,94] from which

the DBH24 subset we had previously used to test barrier heights was taken.[23,101] BHPERI is made up of barrier heights from pericyclic reactions, PX13 and WCPT18 consist of proton-transfer barriers, and BHROT27 includes barriers of rotation.

For these sets, results for B-LYP-osUW12 are positive, errors for BHPERI and BHDIV10 are the lowest of the non-dispersion corrected functionals. Errors for BH76, PX13 and WCPT18 are lower than DSD-BLYP in each case. Though XYGJ-OS gives the lowest errors for BH76 and WCPT18. For PX13, fB-LYP-osUW12 outperforms B-LYP-osUW12, with this functional and DOD-BLYP showing similar errors both within chemical accuracy for this set.

Including dispersion in B-LYP-osUW12 results in minimal improvement with errors increasing slightly for three of the sets. DOD-BLYP in particular shows large improvement with dispersion, with DOD-BLYP(D3BJ) giving the lowest errors for BHPERI, BHDIV10, and PX13.

Overall results for barrier heights are positive. B-LYP-osUW12 gives some of the smallest errors for the non-dispersion functionals for multiple test sets. However, when dispersion is added the errors seem to increase, while for double hybrids errors decrease with dispersion particularly DOD-BLYP(D3BJ).

Reaction energies. Figure 8 shows the errors for six reaction energies test sets. Included in these sets are the BH76RC test contains the reaction energies of the BH76 barrier heights set, the Diels-Alder reaction set DARC, and the G2RC set of reaction from the G2/97 test set, and the set. Also included is the DC13 test set consists of thirteen difficult cases for DFT, this set is an expansion of the earlier DC9 test set from the GMTKN24/30 databases.

Overall, B-LYP-osUW12 gives similar results to DSD-BLYP in most cases. Errors for DARC, FH51, and DC13 are similar for both functionals. While errors for NBPRC are slightly greater for B-LYP-osUW12. For BH76RC, B-LYP-osUW12 falls slightly below the accuracy of the double hybrids hybrid functionals, despite the results for BH76.

For G2RC test set, the errors in the UW12 functionals are shown to be significantly

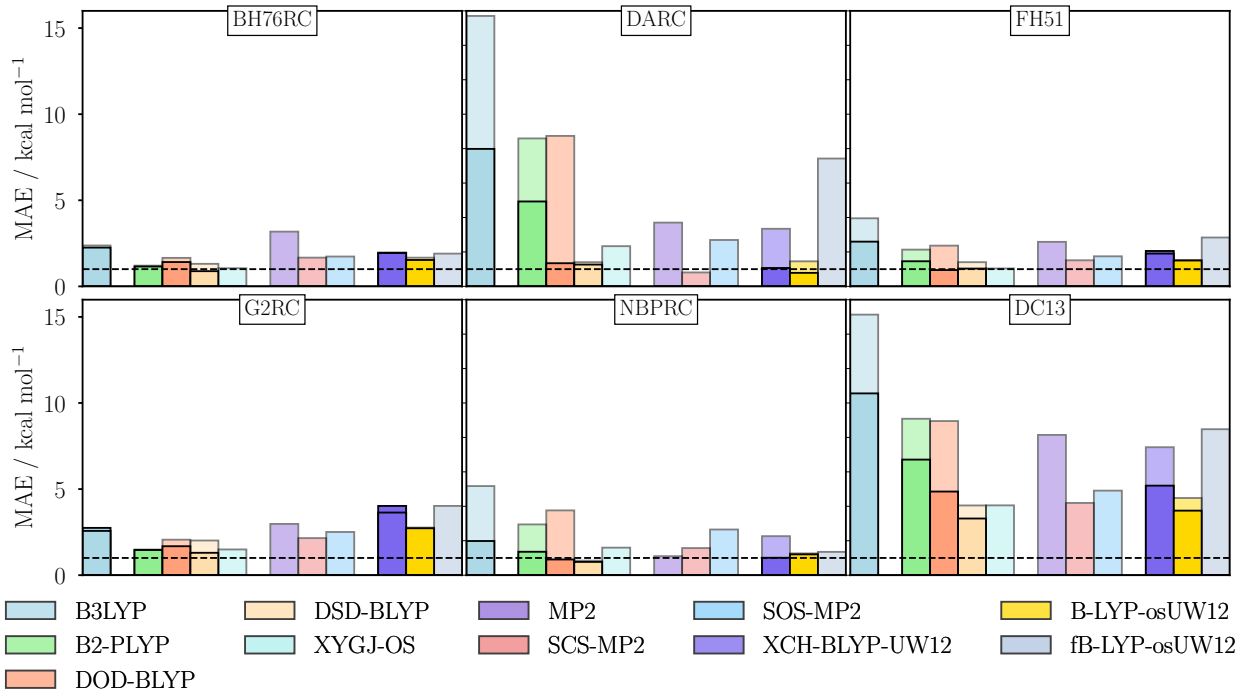

Figure 8: Mean absolute errors (MAE) for the reaction energy test sets BH76RC,[93,94] DARC,[102] FH51,[103,104] G2RC,[61] NBPRC,[43,105,106] and DC13.[17,106] Chemical accuracy (1 kcal mol^{-1}) is indicated by the dotted lines. Dispersion corrected functionals are shown in bold, while uncorrected functionals are translucent.

greater than the other functionals considered, with minimal improvement with dispersion. For this set the error in B-LYP-osUW12 is similar to B3LYP, though it should be noted that B3LYP was optimized on the G2/97 test set from which these reactions are taken.

Re-optimizing with dispersion does not improve results for G2RC, NBPRC, or FH51. For DARC and DC13 errors are reduced for B-LYP-osUW12-D3BJ, which gives the lowest overall errors for DARC. For DC13 the improvement with dispersion is similar for both B-LYP-osUW12 and DSD-BLYP, with errors for B-LYP-osUW12-D3BJ only slightly greater than DSD-BLYP(D3BJ) for this difficult set. Dispersion also greatly improves results for XCH-BLYP-UW12 for the DARC and NBPRC test sets, with XCH-BLYP-UW12-D3BJ resulting in lower errors than B-LYP-osUW12-D3BJ for this set, though DSD-BLYP(D3BJ) shows a slightly lower error.

Overall results for reaction energies show similar levels of accuracy to the double hybrids

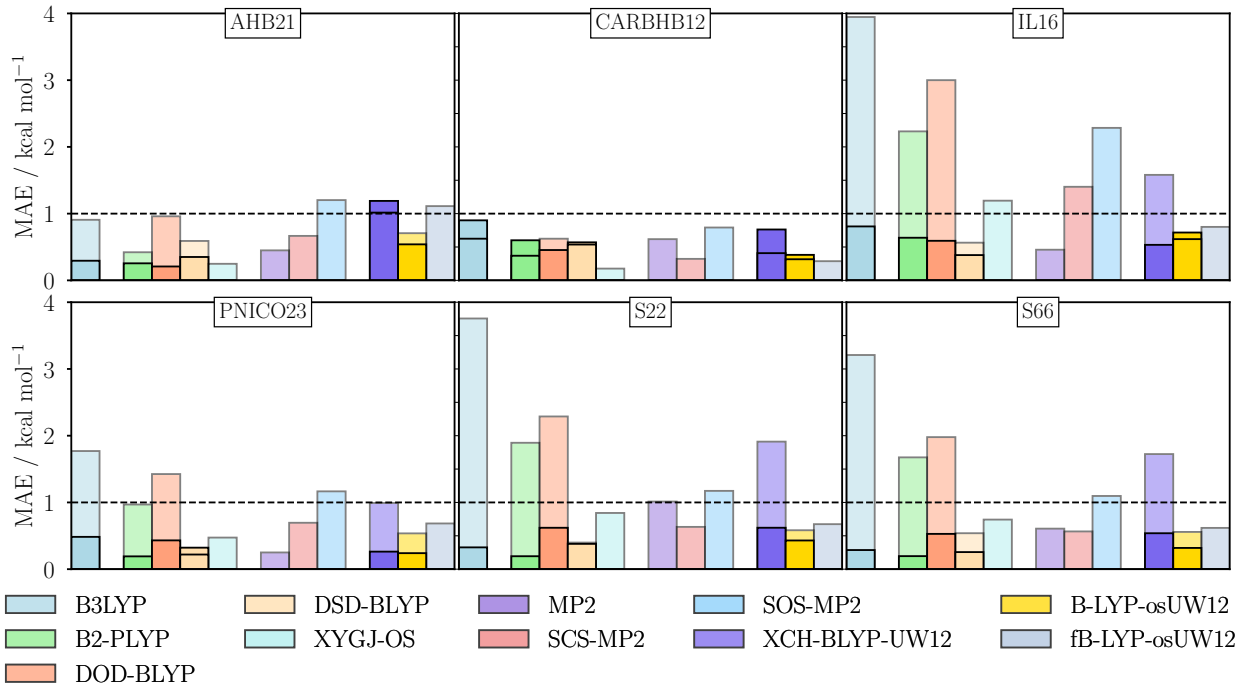

Figure 9: Mean absolute errors (MAE) for the inter-molecular non-covalent interactions test sets AHB21,[81] CARBHB12,[17] IL16,[81] PNICO23,[107] S22,[108] and S66.[109] Chemical accuracy (1 kcal mol^{-1}) is indicated by the dotted lines. Dispersion corrected functionals are shown in bold, while uncorrected functionals are translucent. Calculations use the Def2-QZVP basis except for IL16 and AHB21 which use the aug-cc-pVQZ basis set.

considered. B-LYP-osUW12-D3BJ results in the smallest errors for DARC, and results for NBPRC, FH51, and the DC13 test set are of similar accuracy to the double hybrids. However, for the G2RC test set errors are significantly greater than for double hybrids. By far the most significant error in this set is the reaction $C_6H_6 \longrightarrow 3\,C_2H_2$ which has a much greater error than the remaining reactions which further increases for B-LYP-osUW12-D3BJ.

Inter-molecular non-covalent interactions Figure 9 shows MAEs for six of the inter-molecular non-covalent interaction test sets in GMTKN55. Of these, only S22 is in the training set. B-LYP-osUW12 and B-LYP-osUW12-D3BJ result in errors which are within chemical accuracy for each of these sets. For CARBHB12, the errors in B-LYP-osUW12 and fB-LYP-osUW12 are shown to be lower than significantly lower than DSD-BLYP, with fB-LYP-osUW12 producing the lowest error of the three, though XYGJ-OS gives the lowest error for this set and B2-PLYP produces a similar error to B-LYP-osUW12. For S66 and IL16,

errors for B-LYP-osUW12 and DSD-BLYP are shown to be similar. For AHB21, PNICO23, and S22, errors for B-LYP-osUW12 are slightly larger than DSD-BLYP. For AHB21, B2-PLYP and XYGJ-OS five the lowest errors. MP2 gives the smallest errors for PNICO23. For the S22 set, the errors for B-LYP-osUW12 are smaller than all other zero-dispersion double hybrids.

Adding dispersion improves results for four of the test sets. In particular the error for pnicogen set PNICO23 is greatly reduced with B-LYP-osUW12-D3BJ outperforming DSD-BLYP(D3BJ), though B2-PLYP(D3BJ) gives the lowest errors for this set. Errors are also reduced for S66, though the reduction is not as great as for DSD-BLYP(D3BJ) and B2-PLYP(D3BJ) which result in the lowest errors for this set. For AHB21 some improvement is seen for B-LYP-osUW12-D3BJ, though the error is still greater than the three dispersion-corrected double hybrids. For S22 results are improved for B-LYP-osUW12-D3BJ, with a smaller error than DOD-BLYP(D3BJ), but B2-PLYP(D3BJ), DSD-BLYP(D3BJ), as well as B3LYP(D3BJ) give the lowest errors.

Errors for CARBHB12 are slightly greater for B-LYP-osUW12-D3BJ than B-LYP-osUW12, however all other dispersion corrected functionals except DOD-BLYP(D3BJ) show increased errors compared to the non-dispersion versions. The result is that B-LYP-osUW12-D3BJ has the lowest MAE of the dispersion corrected functionals.

Overall, results for these sets with B-LYP-osUW12 with and without a D3BJ correction are of similar accuracy to the corresponding double hybrid functionals. Including dispersion also results in significant error reduction for four of these set for B-LYP-osUW12.

Intra-molecular non-covalent interactions. Figure 10 shows MAEs for six test sets which study non-covalent intra-molecular interactions. These sets consist of the relative energies of conformers for different types of molecules: ACONF includes alkanes, Amino20x4 - amino acids, BUT14DIOL includes conformers of butane-1,4,diol, ICONF includes inorganic systems, MCONF - melatonin, and SCONF consists of sugar conformers. Overall, small errors are observed for many of these sets.

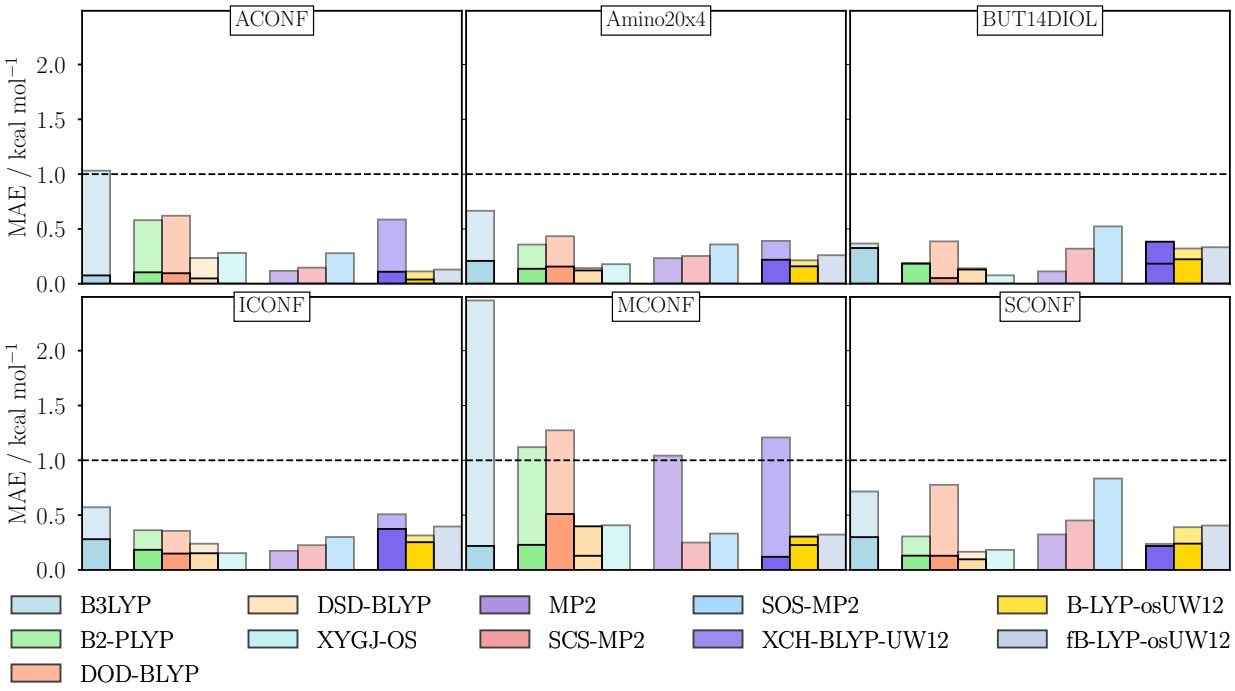

Figure 10: Mean absolute errors (MAE) for the intra-molecular non-covalent interactions test sets ACONF,[110] Amino20x4,[111] BUT14DIOL,[112] ICONF,[17] MCONF,[113] and SCONF.[106] Chemical accuracy ($1\,\mathrm{kcal\,mol^{-1}}$) is indicated by the dotted lines. Dispersion corrected functionals are shown in bold, while uncorrected functionals are translucent.

In each case, B-LYP-osUW12 is an improvement over XCH-BLYP-UW12 and fB-LYP-osUW12. For the ACONF set, errors for B-LYP-osUW12 are less than all other functionals. Results for fB-LYP-osUW12 are also lower than double hybrids, Results for Amino20x4 show B-LYP-osUW12 to be of similar quality to DSD-BLYP and XYGJ-OS the best performers for this set. Errors for BUT14DIOL, and SCONF are greater for B-LYP-osUW12 compared with DSD-BLYP. For ICONF and MCONF errors for B-LYP-osUW12 are greater than DSD-BLYP. For ICONF errors are similar to B2-PLYP, while for MCONF, B-LYP-osUW12 outperforms B2-PLYP, and XYGJ-OS.

Dispersion reduces the error for B-LYP-osUW12 for all sets except MCONF. For ACONF, the MAE for B-LYP-osUW12-D3BJ is less than $0.04\,\mathrm{kcal\,mol^{-1}}$ lower than all other functionals considered, while while XCH-BLYP-UW12-D3BJ has similar errors to B2-PLYP(D3BJ) and DOD-BLYP(D3BJ). For Amino20x4 B-LYP-osUW12-D3BJ results in a similar error to the dispersion-corrected double hybrids. Errors in B-LYP-osUW12 are reduced for BUT14DIOL,

ICONF, and SCONF but not to the same degree as the double hybrids. In particular DOD-BLYP(D3BJ) is shown to give almost negligible error for BUT14DIOL.

For MCONF, errors increase with dispersion for B-LYP-osUW12-D3BJ, though not as great as for DSD-BLYP. The result is that B-LYP-osUW12(D3BJ) shows a lower MAE than DSD-BLYP(D3BJ) for this set. However, both B2-PLYP(D3BJ) and B3LYP(D3BJ) have lower errors, though not as small as XCH-BLYP-UW12-D3BJ has the smallest MAE for this set.

Overall for these sets results for the UW12 functionals are shown to be of a similar level of accuracy to the double hybrid functionals with and without dispersion, particularly for the ACONF, Amino20x4 and MCONF. In cases where the error is slightly greater for B-LYP-osUW12 compared to double hybrids, we note that these are still small errors with the maximum error for B-LYP-osUW12 less than $0.4\,\mathrm{kcal\,mol^{-1}}$ for these sets.

Other properties. Figure 11 shows errors for a selection of test sets covering different properties. The AL2X6 test set includes results for the dimerisation of aluminium compounds. For this set, the dispersion uncorrected UW12 show large errors compared to the DSD-BLYP and XYGJ-OS double hybrids. These results show large improvement with a D3BJ correction, with errors for B-LYP-osUW12-D3BJ lower than B2-PLYP(D3BJ) and DOD-BLYP(D3BJ), though the DSD-BLYP(D3BJ) functional results in the smallest errors for this set. The CDIE20 test set includes results for double bond isomerisations. Errors for B-LYP-osUW12 are similar to DSD-BLYP for this set with and without dispersion. However, the fB-LYP-osUW12 and XYGJ-OS functionals result in the smallest errors for this set. A large fraction of exact exchange seems to be advantageous for this set since the scaled MP2 methods also result in small errors. RSE43 is a radical stabilisation test set. For this set errors the lowest errors are produced by XYGJ-OS, fB-LYP-osUW12, and B-LYP-osUW12. Dispersion has minimal effect on results for this set. For the PArel test set which studies energies of protonated isomers, B-LYP-osUW12 shows similar errors to the double hybrid functionals. Increased errors are seen for fB-LYP-osUW12 and XCH-BLYP-UW12, while

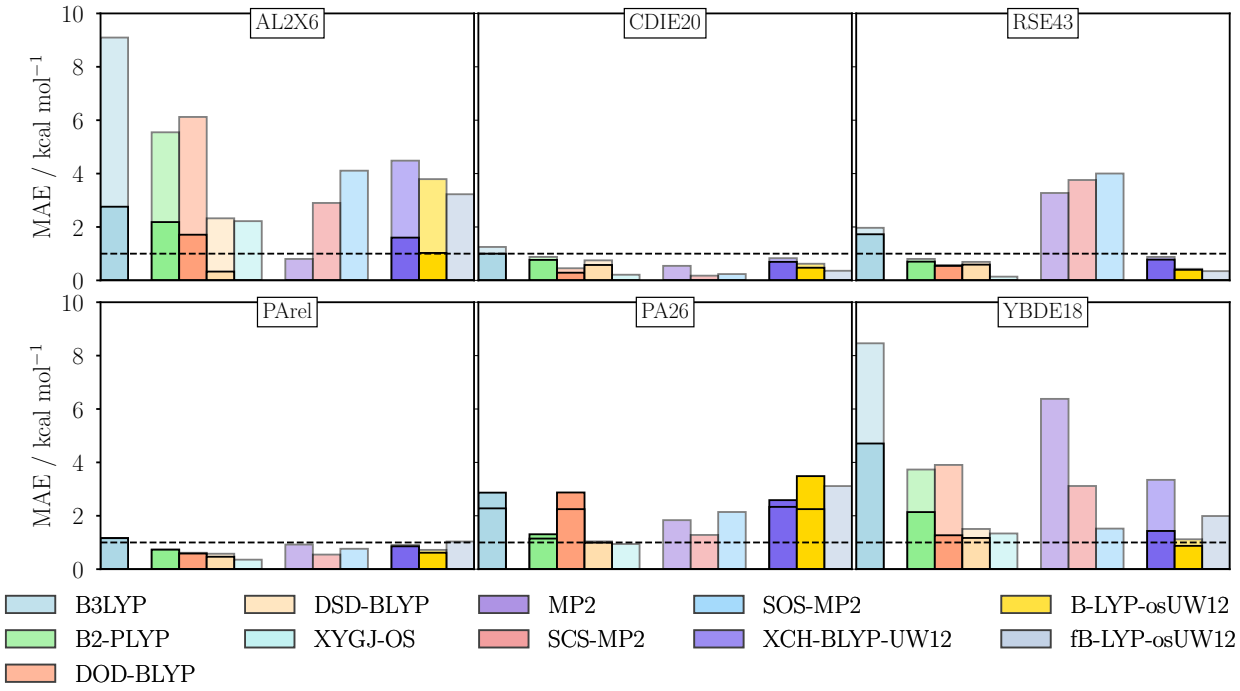

Figure 11: Mean absolute errors (MAE) for the test sets AL2X6,[17] CDIE20,[114] RSE43,[13] PArel,[17] PA26[17,115,116] and YBDE18.[117] Chemical accuracy ($1\,\mathrm{kcal\,mol^{-1}}$) is indicated by the dotted lines. Dispersion corrected functionals are shown in bold, while uncorrected functionals are translucent.

XYGJ-OS produces the smallest errors. The PA26 proton affinity test set is an expansion of the earlier PA set used in the fitting. Errors for UW12 functionals are greater than for the double hybrids except DOD-BLYP. Errors are further increased with a D3BJ correction. For the YBDE18 test set of bond-dissociation energies in ylides, the B-LYP-osUW12 functional results in lower errors than both DSD-BLYP and XYGJ-OS. This is further improved with dispersion, with B-LYP-osUW12-D3BJ achieving chemical accuracy with errors lower than both DOD-BLYP(D3BJ) and DSD-BLYP(D3BJ) which show similar results.

Mindless Benchmarking. The test set which results in the greatest error for B-LYP-osUW12 functionals compared to DSD-BLYP is by far the 'mindless-benchmarking' test set MB16-43[17] This set consists of reactions involving randomly created structures designed to remove bias which may be present in other test sets. This set replaces the MB08-165 test set from GMTKN30.[118] Figure 12 shows the results for both these sets. For the original MB08-

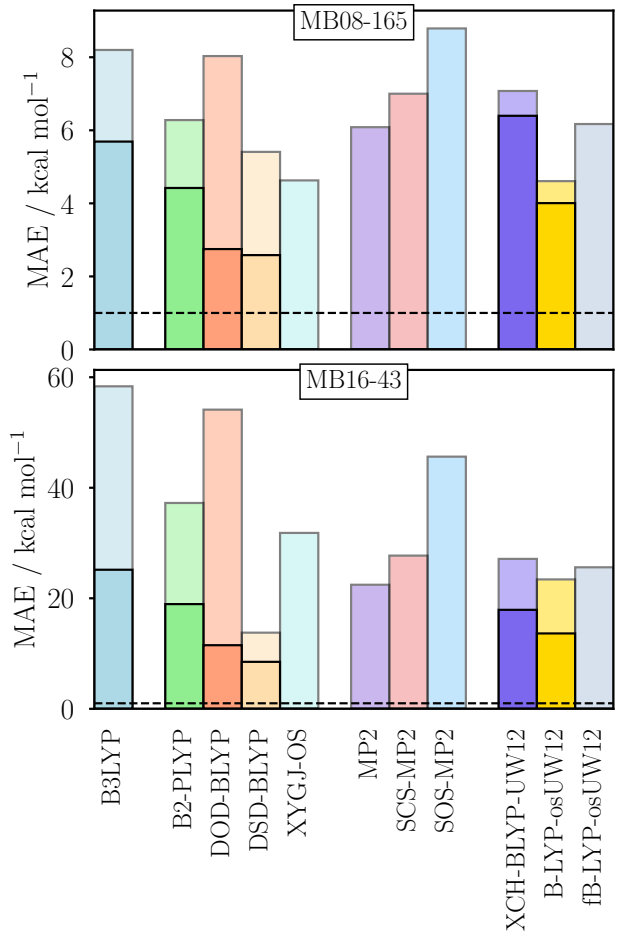

Figure 12: Mean absolute errors (MAE) for the 'mindless benchmarking' test sets MB08-165 and MB16-43 from the GMTKN30 and GMTKN55 databases respectively. Chemical accuracy ($1\,\mathrm{kcal\,mol^{-1}}$) is indicated by the dotted lines. Dispersion corrected functionals are shown in bold, while uncorrected functionals are translucent.

165 test set, which was used in the optimization of the new functionals, B-LYP-osUW12 outperforms all the non-dispersion corrected functionals. Addition of dispersion results in minimal change in the UW12 results for MB08-165 while the dispersion-corrected double hybrids show significant improvement results in the smallest error for DSD-BLYP(D3BJ). For the newer MB16-43 errors are significantly greater, however DSD-BLYP results in much lower errors than all other functionals considered with and without dispersion. The error for B-LYP-osUW12 is significantly greater than for DSD-BLYP, though this difference is significantly reduced by dispersion.

Atomization Energies. Figure 13 shows the mean absolute errors for the W4-11 atom-

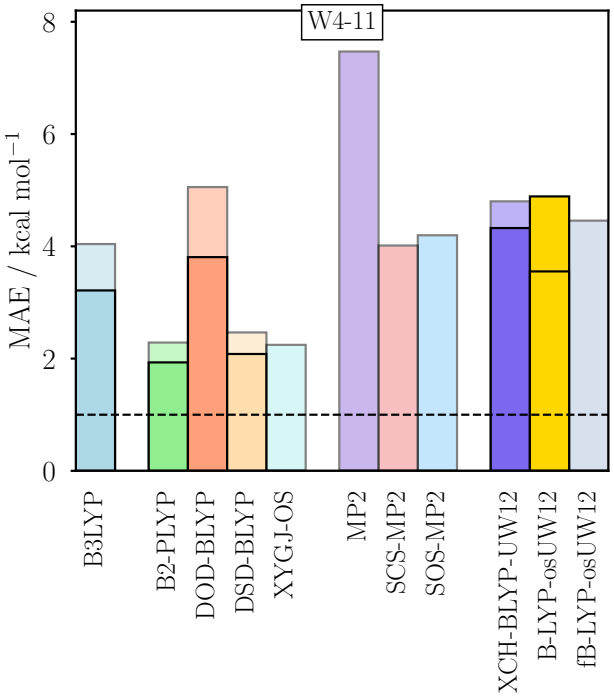

Figure 13: Mean absolute errors (MAE) for the atomization energy test set W4-11.[119] Chemical accuracy (1 kcal mol^{-1}) is indicated by the dotted lines. Dispersion corrected functionals are shown in bold, while uncorrected functionals are translucent.

ization energies test set. This set replaces the W4-08 set from the GMTKN30 database used in the fitting.[120] B-LYP-osUW12 shows significantly greater errors than B2-PLYP, DSD-BLYP and XYGJ-OS, with an error similar to B3LYP. This error significantly increases when dispersion is added, with the error for B-LYP-osUW12 greater than for both fB-LYP-osUW12 and XCH-BLYP-UW12.

Significant errors. Figure 14 shows results for the other test sets which result in the largest errors for B-LYP-osUW12 compared with DSD-BLYP. Of these, both ALK8 and ALKBDE10 cover the dissociation of alkaline compounds; G21IP, DIPCS10, and G21EA measure ionization potentials and electron affinities; and SIE4x4 contains self-interaction related problems. For all of these sets except ALK8, the dispersion corrected B-LYP-osUW12-D3BJ results in greater errors than B-LYP-osUW12. For SIE4x4, the error is directly related to the fraction of exact exchange in the functional with similar errors for B2-PLYP, XCH-BLYP-UW12, and B-LYP-osUW12. This error is significantly reduced by the fixed fraction

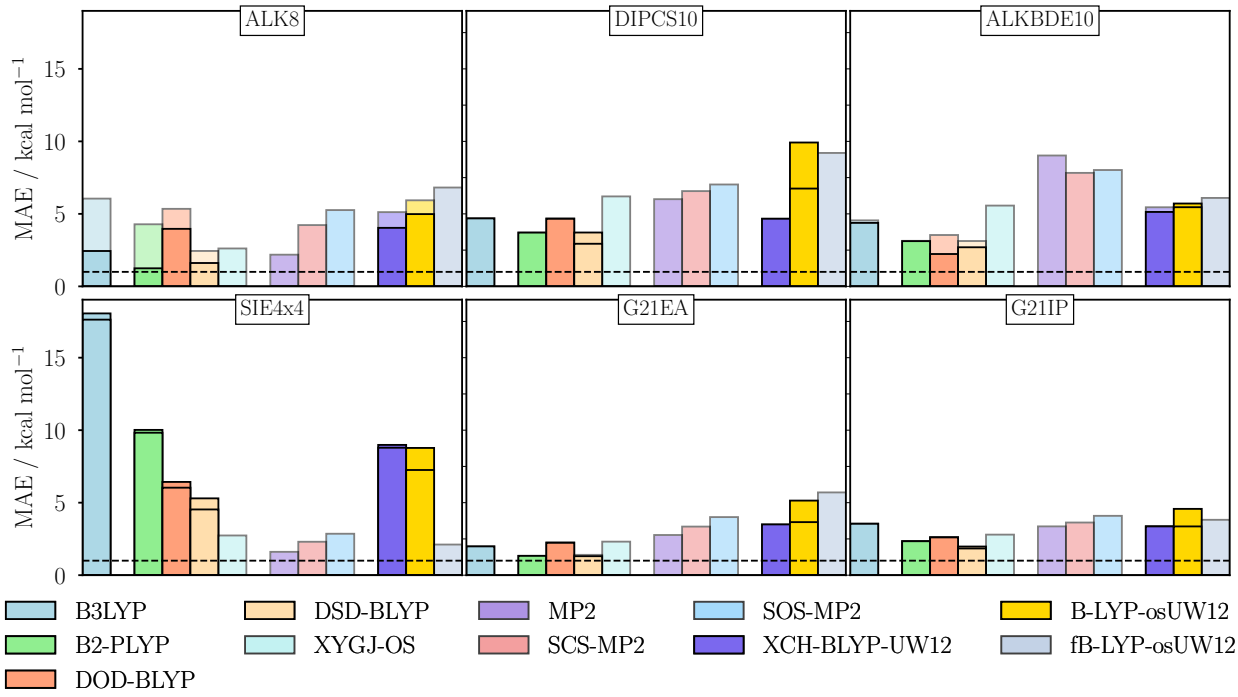

Figure 14: Plots showing the mean absolute errors (MAEs) for six test sets ALK8,[17] DIPCS10,[17] ALKBDE10,[121] SIE4x4,[17] G21EA,[80] G21IP.[80] Chemical accuracy (1 kcal mol^{-1}) is indicated by the dotted lines. Dispersion corrected functionals are shown in bold, while uncorrected functionals are translucent.

fB-LYP-osUW12 which shows lower errors than all the double hybrids. This will be discussed further in section 4.3.

For the double ionization potential test set DIPCS10, both B-LYP-osUW12 and fB-LYP-osUW12 result in much larger errors than the double hybrid functionals. The dispersion uncorrected B-LYP-osUW12 shows significant improvement over B-LYP-osUW12-D3BJ, but still results in larger errors than the double hybrid functionals. The XCH-BLYP-UW12 functional results in a significantly lower error than B-LYP-osUW12 with a similar error to DOD-BLYP for this test set.

For G21IP, the largest errors for B-LYP-osUW12 and fB-LYP-osUW12 the largest errors are the ionization of Be and Mg. This is indicative a general trend since three of these sets contain results for group 1 and 2 atoms and molecules. The largest errors for B-LYP-osUW12 for ALK8 are for the reactions $Li_8 \longrightarrow 4\,Li_2$ and $Na_8 \longrightarrow 4\,Na_2$. Of all the test sets in

GMTKN55, these ones as well as MB16-43 contain significant numbers of reactions involving group s-block elements and compounds. This may indicate that the B-LYP-osUW12 functional may be less accurate for these systems, which could be related to the single range parameter r_c used in the geminal function.

Overall, B-LYP-osUW12 offers a large improvement over XCH-BLYP-UW12, with improved results for 39 of the 44 test sets from the GMTKN55 database. While fB-LYP-osUW12 also shows improvement for a number of test sets – offering increased performance for 25 out of the 44 test sets considered. The dispersion corrected B-LYP-osUW12 also shows large improvements over XCH-BLYP-UW12-D3BJ with improved results for 32 of the 44 sets considered.

Of the non-dispersion corrected double-hybrid methods considered, DSD-BLYP and XYGJ-OS give the best results overall. These two methods give similar results for many test sets. DSD-BLYP results in particularly small errors for the 'mindless benchmark' MB16-43 set, the NBPRC reaction energies set, non-covalent interaction S22 and S66 sets. Both give similar results for the difficult cases in DFT set (DC13). XYGJ-OS performs significantly better for barrier heights, the original 'mindless-benchmark' set of decompositions (MB08-165), and the self-interaction test set (SIE11). These double hybrids offer significant improvement over B2-PLYP, with reduced errors across most of the test sets considered. However, B2-PLYP is better than both DSD-BLYP and XYGJ-OS for atomization energies.

It should be noted that double hybrids are outperformed by the (scaled) MP2 methods for some of the test sets – notably the DARC reaction energy set, the pnicogen dimer set PNICO23, and self-interaction error set (SIE4x4).

The dispersion-uncorrected B-LYP-osUW12 functional offers double-hybrid level results for many properties, with errors comparable to both DSD-BLYP and XYGJ-OS for a number of test sets. Results also improve upon these double hybrid functionals in some areas. In particular, results for conformers (ACONF), barrier heights (BHPERI), bond separation reactions (BSR36), and dissociation (YBDE18) show improved results compared to these

double hybrids. Additionally, results for barrier heights (BH76, BHDIV10), radical stabilizations (RSE43), non-covalent binding energies (IL16, S22, S66), and the NBPRC reaction energies set result in similar or improved results to these double hybrids. While errors for atomization energies (W4-11) are not as low as for some of the double hybrids, B-LYP-osUW12 demonstrates similar accuracy to hybrid functionals, with errors lower than B3LYP. Also, while errors for NBPRC and DARC reaction energy sets are similar to double hybrids, errors are somewhat increased for the other reaction energy sets; G2RC and BH76RC. The test sets where the functional has particularly large errors in comparison to double hybrids are the mindless benchmarking set MB16-43, reactions involving alkaline compounds (ALK8/ALKBDE10), proton affinities (PA26), and ionization potentials (G21IP/DIPCS10). Also it should be noted that results for the difficult cases for DFT (DC13) show reasonable errors similar to most of the double hybrids.

Since we have fixed one of the parameters in fB-LYP-osUW12 compared with B-LYP-osUW12, we would automatically expect errors to increase compared to B-LYP-osUW12. However, the functional performs better than B-LYP-osUW12 for seven test sets: the dimerization of Al compounds (AL2X6), double bond isomerisations (CDIE20), tautomers (TAUT15), proton-exchange barriers (PX13), reaction separation energies (RSE43), hydrogen bonding (CARBHB12), and self-interaction errors SIE4x4. Similar results are observed for conformers (ACONF/MCONF/SCONF), non-covalent interactions (S66/Amino20x4/IL16), and reaction energies (BH76RC/NBPRC). The most significant increases in errors compared with B-LYP-osUW12 occur for the DARC reaction energy test set and the DC13 difficult cases for DFT set. Significant increases in error are also seen observed for barrier heights (BH76, BHPERI), bond separation reactions (BSR36), other reaction energies (particularly G2RC and FH51), and atomization energies (W4-11).

Re-optimizing B-LYP-osUW12 with a D3BJ dispersion correction improves results for 28 of the 44 test sets considered. Significant improvements are seen for the difficult cases for DFT set (DC13), non-covalent sets (PNICO23, S66, SCONF), aluminium dimer set

(AL2X6), and the mindless benchmark set (MB16-43). However, the B-LYP-osUW12-D3BJ also results in much larger errors for a number of sets compared to B-LYP-osUW12 including electron affinities (G21EA), atomization energies (W4-11), proton affinities (PA26), ionization potentials (G21IP/DIPCS10) and self-interaction errors (SIE4x4). Overall, the improvement in results for B-LYP-osUW12 compared to DSD-BLYP re-optimized for dispersion is significantly smaller. For a number of test sets including WCPT18, IL16, W4-11, and ALKBDE10 other functionals show reduced errors using the dispersion-corrected functionals, while the error for B-LYP-osUW12 increases. B-LYP-osUW12 does outperform all the dispersion-corrected hybrids for a number of test sets, notably ACONF, PNICO23, RSE43, CARBHB12, DARC, and YBDE18. However, we must note that empirical dispersion corrections and their damping have been designed to work with standard density functionals; the damping has not been designed to work with UW12 correlation, which may explain the small improvement compared to other methods.

Examining the effect of orbital optimization on the results for the UW12 functionals. In most cases the change in results due to orbital optimization is minimal, with $\Delta\text{MAE} < 0.1\,\text{kcal}\,\text{mol}^{-1}$ for most of the GMTKN30 test sets. Figure 15 show the change in the MAE for test set in the GMTKN30 database used, for the non-dispersion corrected functionals. The sets shown are the ones for which at least one of the functionals shows a difference of at least $0.1\,\text{kcal}\,\text{mol}^{-1}$. For B-LYP-osUW12 the only notable differences occur in results for BHPERI, DARC, O3ADD6, and SIE11, of which only BHPERI and DARC appear in the GMTKN55 database. Results for BHPERI are slightly improved by optimization, while for the O3ADD6 set errors increase slightly with optimization. Similar changes are observed for XCH-BLYP-UW12, which also sees a noticeable decrease in RMSE for the DC9 test set. In both these cases all changes except for O3ADD6 with B-LYP-osUW12 are less than $0.14\,\text{kcal}\,\text{mol}^{-1}$ ($|\Delta\text{MAE}|_{\text{B-LYP-osUW12}} = -0.29\,\text{kcal}\,\text{mol}^{-1}$). For fB-LYP-osUW12, greater changes are observed for most test sets, notably BH76 and O3ADD6. This is most likely due to the fB-LYP-osUW12 optimized orbitals being significantly different from the B3LYP

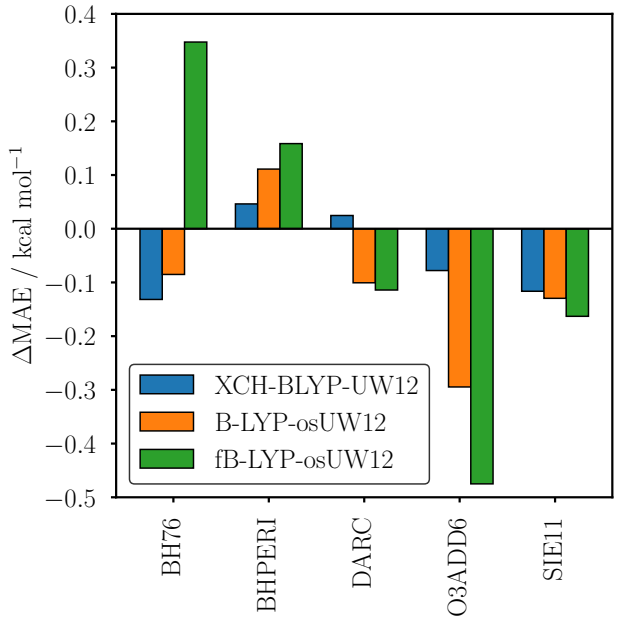

Figure 15: Plot showing the change in MAE error for test sets in the GMTKN30 database, where energies are calculated using B3LYP orbitals with the fully self-consistent functional as reference. These test sets[93–98,102,106,122] are the ones for which at least one of the functionals shows an error of 0.1 kcal mol^{-1} or more.

optimized orbitals resulting from the high fraction of exact exchange. However, these energy differences are still relatively small compared to the overall errors.

Overall, the B-LYP-osUW12 functional has been shown to produce accurate results for conformers, barrier heights, bond separation reactions, isomerizations, and selected reaction energies. In addition, where results are not as accurate as double hybrids, such as atomization energies and some other reaction energies, the errors are similar to those of standard hybrid functionals. The functional gives reasonable results for cases which are notably difficult for DFT. Addition of dispersion to B-LYP-osUW12-D3BJ improves results for a number of test sets, particularly those involving long-range behaviour. However in many cases results are not improved significantly and errors are increased. Overall the dispersion functional outperforms the non-dispersion version, though the functional is not always as accurate as similar dispersion corrected double hybrids. The fB-LYP-osUW12 functional offers some improvement over the B-LYP-osUW12 functional for a small number of test sets, notably those susceptible to self-interaction errors. However, in general the functional does not

produce as accurate results as B-LYP-osUW12 for most test sets. While some of these increased errors are small, there are a number of test sets for which the errors significantly increase.

4.3 Self-Interaction Error

With the new functionals B-LYP-osUW12 and fB-LYP-osUW12, we wish to examine the effect of large fractions of exact exchange on both the self-interaction error and the delocalization error. In this section we look at the non-dispersion corrected version of the functionals.

The errors for this test set are represented visually in figure 16. From these plots it can be immediately seen that B3LYP systematically over-binds the molecular dimers, while for the many-electron systems HF under-binds the dimers. In each case, the two opposite spin only functionals with the greatest fraction of exact exchange XYGJ-OS and fB-LYP-osUW12 result in the lowest errors. DSD-BLYP which also contains a high fraction of exact exchange, has greater errors for the $NH_3 \cdots NH_3{}^+$ and $H_2O \cdots H_2O^+$ dimers. Results for B-LYP-osUW12 show a general improvement over XCH-BLYP-UW12, B-LYP-osUW12 outperforms DSD-BLYP for the two larger systems, while having greater errors for the two smaller systems ($H \cdots H^+$ and $He \cdots He^+$).

For the multi-electron systems, errors are relatively constant with separation distance r, especially for both fB-LYP-osUW12 and XYGJ-OS. For the single-electron system, errors increase with separation distance. Note that in this case, the MP2/UW12 contribution is zero in each of the hybrid functionals. Overall, increased exact exchange is shown to be beneficial in reducing the self-interaction error for both double and UW12 hybrid functionals.

To demonstrate the effect on delocalization error, figure 17 shows the energies of atomic ions with fractional charge. In each case the spin $2S = N_{\mathrm{el},\uparrow} - N_{\mathrm{el},\downarrow}$ for each ion with an integer number of electrons N_{el} was chosen to equal that of the ground-state spin of the neutral atom with the same number of electrons N_{el}. The fractional spin values are

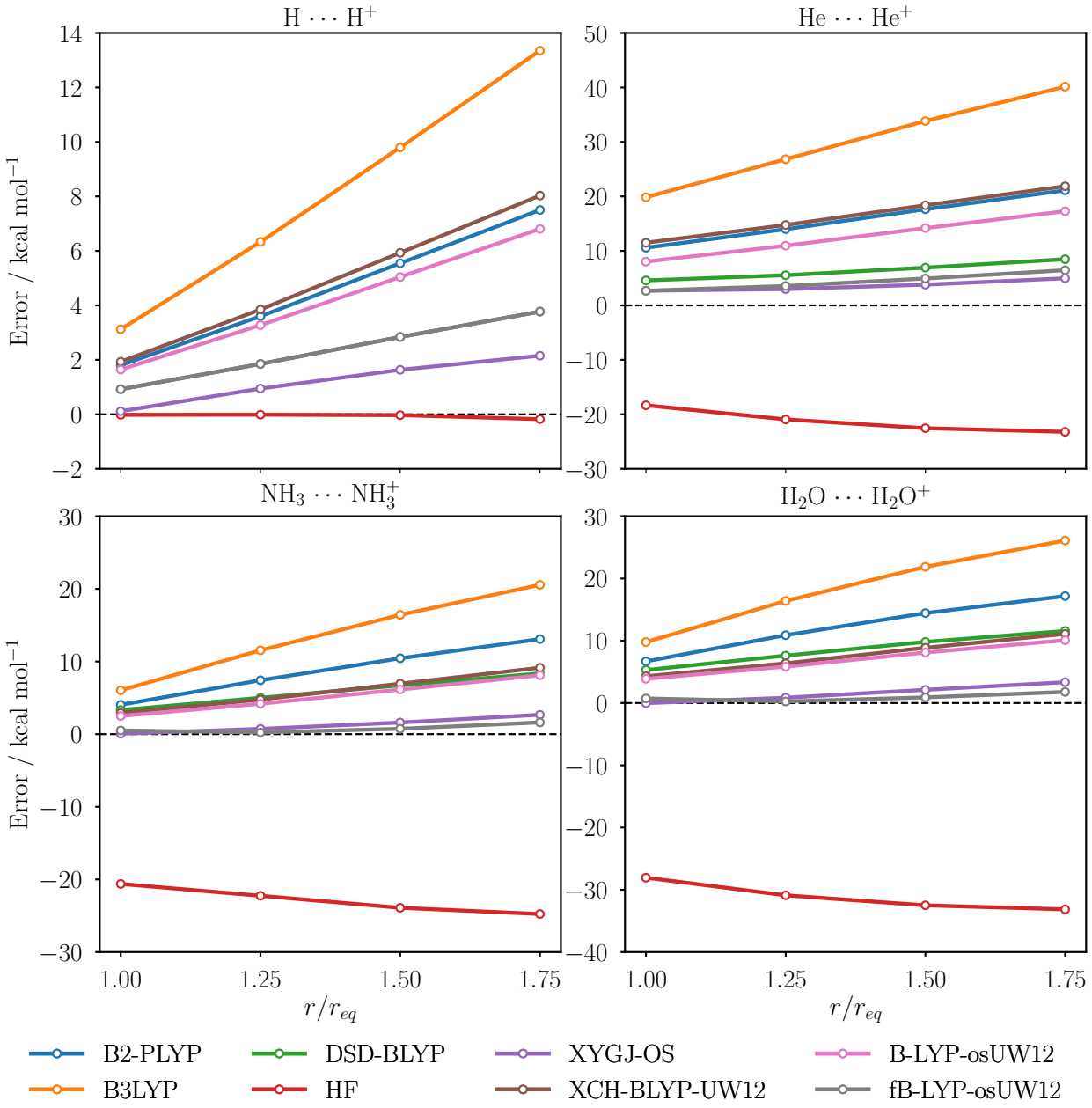

Figure 16: Errors for the SIE4x4 test set for each dimer as a function of dimer separation distance r, in units of equilibrium separation distance r_{eq}. All results are fully self-consistent, calculated using the Def2-QZVP basis set. Reference data is taken from Ref. 17, calculated using W2-F12. For H_2^+, the reference energies are equal to the Hartree-Fock values at the complete basis set limit (HF/CBS). Since HF is exact for H_2^+, any errors in this result are entirely due to incomplete basis set.

then a linear interpolation between the ions of integer charge. This is equivalent to the highest occupied spin-orbital to be fractionally occupied.[123] No spherical orbital symmetry

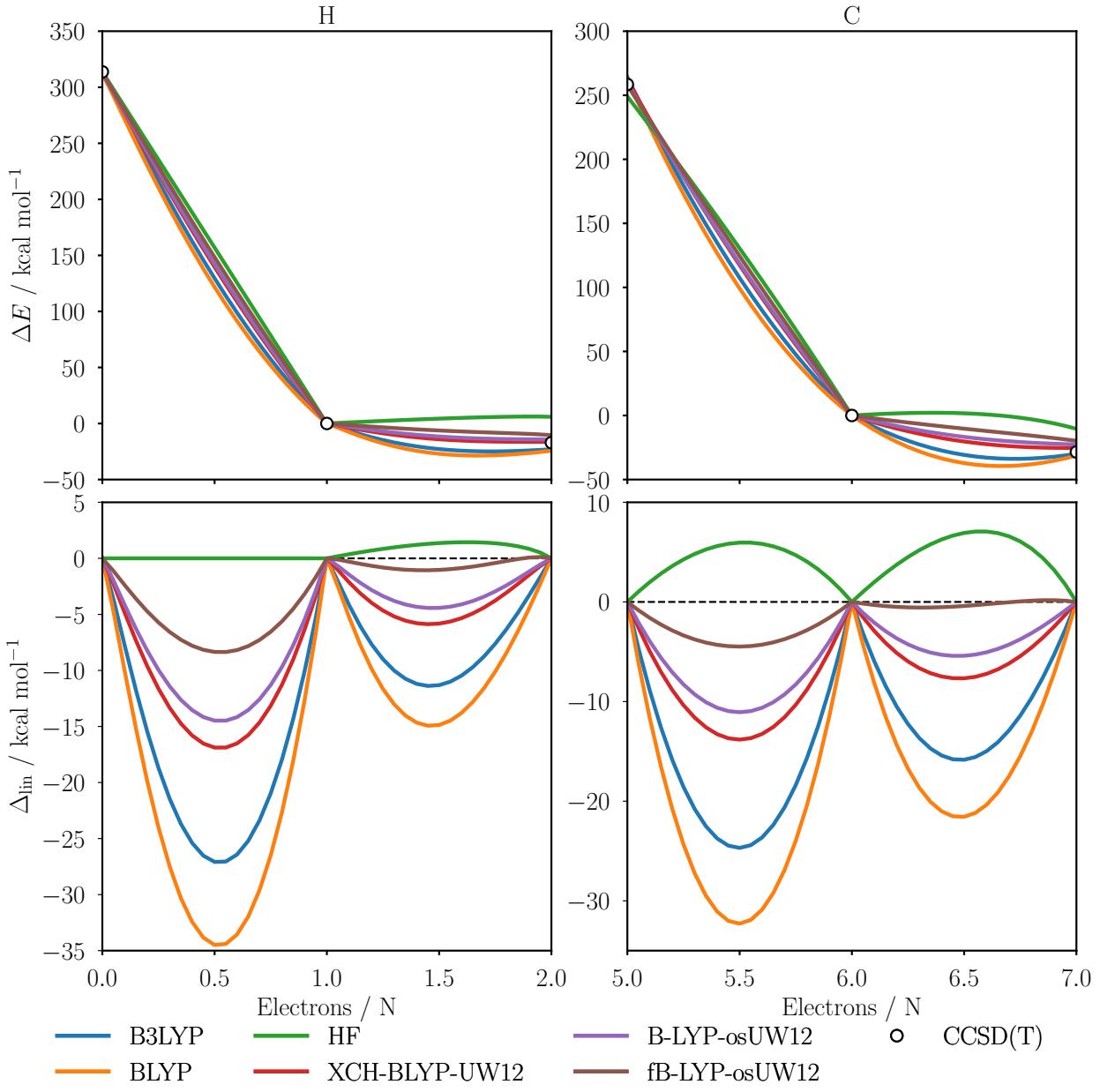

Figure 17: Plots of energy as a function of electron number for atomic ions of Hydrogen and Carbon calculated using multiple hybrid functionals. Results were calculated using the aug-cc-pV(Q+d)Z basis set. The upper plots show the energy relative to the neutral atom ΔE, with the reference CCSD(T) energies at integer values. Note that for Hydrogen, HF is exact up to one electron, while CCSD is exact for H^- with no triples contribution. The lower plots show the deviation from linearity Δ_{lin} calculated using the integer values for each functional.

is imposed, so the highest occupied spin-orbital is never degenerate with other orbitals.

In figure 17 we look at atomic ions of H and C, since it is known that the delocal-

ization error for $H^{0.5+}$ is density-driven, whereas for $H^{0.5-}$, $C^{0.5+}$, and $C^{0.5-}$ the error is energy-driven.[11,21] Also, for the $H^{0.5+}$ section of the curve, there is zero UW12 contribution. For XCH-BLYP-UW12, the deviation from linearity for $C^{0.5+}$ is $-13.82\,\mathrm{kcal\,mol^{-1}}$ which is similar to the literature value for B2-PLYP ($\Delta_{\mathrm{lin}}(5.5) = -14\,\mathrm{kcal\,mol^{-1}}$).[124] For this value, B-LYP-osUW12 shows a slight improvement with $\Delta_{\mathrm{lin}}(5.5) = -11.07\,\mathrm{kcal\,mol^{-1}}$, while fB-LYP-osUW12 results in an error of $\Delta_{\mathrm{lin}}(5.5) = -4.48\,\mathrm{kcal\,mol^{-1}}$. This value is comparable to the value for XYGJ-OS from the literature ($\Delta_{\mathrm{lin}}(5.5) = -3.5\,\mathrm{kcal\,mol^{-1}}$), for which the smaller deviation is due to the higher fraction of exact exchange in XYGJ-OS.

5 Conclusions

In this paper we have shown that it is possible to use the UW12 approximation with a one-parameter Slater-type geminal function to achieve MP2 level accuracy for the correlation energy. Using this approximation hybrid exchange-correlation functionals have been constructed with accuracy across a broad range of test sets that is close to that of modern double hybrids.

We created new functionals B-LYP-osUW12 and fB-LYP-osUW12 containing only opposite spin UW12 correlation and optimized the parameters using tests sets from the GMTKN30 database. The resulting functionals both contain a larger fraction of exact exchange than the previous XCH-BLYP-UW12 functional, with a range parameter r_c larger than previously used. We also re-optimized B-LYP-osUW12 with a D3BJ dispersion correction using the same method. The optimal range parameter for this functional is the same as the one previously used for XCH-BLYP-UW12.

Using test sets from the GMTKN55 database, we showed that B-LYP-osUW12 is more accurate than XCH-BLYP-UW12 for many of the test sets considered, producing results of double hybrid level accuracy for a number of properties including barrier heights and bond separation reactions. Reasonable results are also achieved for reaction energies and

atomization energies.

We demonstrated the effect of a large fraction of exact exchange by creating the fB-LYP-osUW12 functional with a fixed fraction of 75% exact exchange. This resulted in improved results for self-interaction related problems, dimerization of aluminium compounds and radical stabilization energies. It also reduced the dissociation errors present in fractionally charged systems. Though this also resulted in an increase in error for many test sets, particularly reaction energies and atomization energies.

We looked at the effect of dispersion on results and found that our dispersion-corrected functional B-LYP-osUW12-D3BJ showed reduced errors for a number of test sets. Though we showed that in many cases results show minimal improvement or increased error compared to B-LYP-osUW12. We believe this is due to the difference length scales of the geminal operator and the damping in D3BJ which is designed to work with DFT and r_{12}^{-1} potentials. In future we wish to determine the best approach for incorporating dispersion effects with UW12 correlation, for instance using the D4 dispersion model or screening the coulomb operator in the UW12 correlation.

However, we have demonstrated excellent results for the B-LYP-osUW12 hybrid which has a similar accuracy overall to the double hybrid functionals considered, containing the same number of parameters but with no dependence on the virtual orbitals. Future developments such as including range-separated exchange can be used to further improve results while reducing the self-interaction error.

In this paper we have focussed on BLYP-based functionals, and while DSD-BLYP(D3BJ) has previously been shown to be among the most accurate double hybrids (particularly for BLYP-based double hybrids). In the original GMTKN55 paper, DSD-BLYP(D3BJ) had the smallest WTMAD-2 value of all functionals considered.[17] The most accurate hybrid functional in that paper was shown to be ωB97X-V for which wMAE is 4.2 kcal mol^{-1}, greater than B-LYP-osUW12-D3BJ.[17,125] More recent double hybrids have been able to achieve even lower errors, such as the recent DSD type hybrid revDSD-PBEP86-D4 for which wMAE =

$2.5\,\mathrm{kcal\,mol^{-1}}$,[126] such functionals have tended to use density-functional exchange-correlation other than BLYP. We believe by considering other exchange-correlation functionals, as well as further studies of the geminal function and dispersion correction, we will be able to further increase the performance of UW12 hybrids to achieve similar levels of accuracy. We also hope to expand our investigation to include transition metal chemistry, where double hybrids are known to be deficient.[17]

Supporting Information Available

The following files are included for additional information:

- supplementary_information.xlsx
- G2-97_geometries.txt: Geometries for the molecules from the G2/97 test set used.
- GMTKN30_B3LYP_Def2-QZVP_components.xlsx: Tables detailing the individual energy contributions for each component used to optimize the UW12 functionals for all test sets and molecules included.
- GMTKN30_energies.xlsx: Calculated energies for all systems for each functional in every included test set from the GMTKN30 database.
- GMTKN30_relative_energies.xlsx: Relative energies for each functional in every included test set from the GMTKN30 database.
- GMTKN55_energies.xlsx: Calculated energies for all systems for each functional in every included test set from the GMTKN55 database.
- GMTKN55_relative_energies.xlsx: Energies for each functional in every included test set from the GMTKN55 database.

Conflict of interest

FRM is Cofounder and CTO of Entos Inc.

Acknowledgement

TCW and ZMW are funded through the Engineering and Physical Sciences Research Council (EPSRC) Centre for Doctoral Training in Theory and Modelling in Chemical Sciences (Grant EPSRC EP/L015722/1).

References

(1) Hohenberg, P.; Kohn, W. Inhomogeneous Electron Gas. *Phys. Rev.* **1964**, *136*, B864–B871.

(2) Kohn, W.; Sham, L. J. Self-consistent equations including exchange and correlation effects. *Phys. Rev.* **1965**, *140*, A1133–A1138.

(3) Seidl, A.; Görling, A.; Vogl, P.; Majewski, J. A.; Levy, M. Generalized Kohn-Sham schemes and the band-gap problem. *Phys. Rev. B* **1996**, *53*, 3764–3774.

(4) Perdew, J. P. Jacob's ladder of density functional approximations for the exchange-correlation energy. AIP Conf. Proc. 2001; pp 1–20.

(5) Becke, A. D. A new mixing of Hartree–Fock and local density-functional theories. *J. Chem. Phys.* **1993**, *98*, 1372–1377.

(6) Görling, A.; Levy, M. Correlation-energy functional and its high-density limit obtained from a coupling-constant perturbation expansion. *Phys. Rev. B* **1993**, *47*, 13105–13113.

(7) Görling, A.; Levy, M. Exact Kohn-Sham scheme based on perturbation theory. *Phys. Rev. A* **1994**, *50*, 196–204.

(8) Eshuis, H.; Bates, J. E.; Furche, F. Electron correlation methods based on the random phase approximation. *Theor. Chem. Acc.* **2012**, *131*, 1084.

(9) Grimme, S. Semiempirical hybrid density functional with perturbative second-order correlation. *J. Chem. Phys.* **2006**, *124*, 034108.

(10) Zhang, Y.; Xu, X.; Goddard, W. A. Doubly hybrid density functional for accurate descriptions of nonbond interactions, thermochemistry, and thermochemical kinetics. *Proc. Natl. Acad. Sci. U. S. A.* **2009**, *106*, 4963–4968.

(11) Su, N. Q.; Xu, X. The XYG3 type of doubly hybrid density functionals. *Wiley Interdiscip. Rev.: Comput. Mol. Sci.* **2016**, *6*, 721–747.

(12) Lochan, R. C.; Head-Gordon, M. Orbital-optimized opposite-spin scaled second-order correlation: An economical method to improve the description of open-shell molecules. *J. Chem. Phys.* **2007**, *126*, 164101.

(13) Neese, F.; Schwabe, T.; Kossmann, S.; Schirmer, B.; Grimme, S. Assessment of orbital-optimized, spin-component scaled second-order many-body perturbation theory for thermochemistry and kinetics. *J. Chem. Theory Comput.* **2009**, *5*, 3060–3073.

(14) Peverati, R.; Head-Gordon, M. Orbital optimized double-hybrid density functionals. *J. Chem. Phys.* **2013**, *139*, 024110.

(15) Sancho-García, J. C.; Pérez-Jiménez, A. J.; Savarese, M.; Brémond, E.; Adamo, C. Importance of Orbital Optimization for Double-Hybrid Density Functionals: Application of the OO-PBE-QIDH Model for Closed- and Open-Shell Systems. *J. Phys. Chem. A* **2016**, *120*, 1756–1762.

(16) Najibi, A.; Goerigk, L. A Comprehensive Assessment of the Effectiveness of Orbital Optimization in Double-Hybrid Density Functionals in the Treatment of Thermochemistry, Kinetics, and Noncovalent Interactions. *J. Phys. Chem. A* **2018**, *122*, 5610–5624.

(17) Goerigk, L.; Hansen, A.; Bauer, C.; Ehrlich, S.; Najibi, A.; Grimme, S. A look at the density functional theory zoo with the advanced GMTKN55 database for general main group thermochemistry, kinetics and noncovalent interactions. *Phys. Chem. Chem. Phys.* **2017**, *19*, 32184–32215.

(18) Kurlancheek, W.; Head-Gordon, M. Violations of N-representability from spin-unrestricted orbitals in Møller-Plesset perturbation theory and related double-hybrid density functional theory. *Mol. Phys.* **2009**, *107*, 1223–1232.

(19) Mori-Sánchez, P.; Cohen, A. J.; Yang, W. Many-electron self-interaction error in approximate density functionals. *J. Chem. Phys.* **2006**, *125*, 201102.

(20) Mori-Sánchez, P.; Cohen, A. J.; Yang, W. Localization and Delocalization Errors in Density Functional Theory and Implications for Band-Gap Prediction. *Phys. Rev. Lett.* **2008**, *100*, 146401.

(21) Perdew, J. P.; Parr, R. G.; Levy, M.; Balduz, J. L. Density-functional theory for fractional particle number: Derivative discontinuities of the energy. *Phys. Rev. Lett.* **1982**, *49*, 1691–1694.

(22) Mardirossian, N.; Head-Gordon, M. Thirty years of density functional theory in computational chemistry: an overview and extensive assessment of 200 density functionals. *Mol. Phys.* **2017**, *115*, 2315–2372.

(23) Wiles, T. C.; Manby, F. R. Wavefunction-like Correlation Model for Use in Hybrid Density Functionals. *J. Chem. Theory Comput.* **2018**, *14*, 4590–4599.

(24) Klopper, W.; Manby, F. R.; Ten-No, S.; Valeev, E. F. R12 methods in explicitly correlated molecular electronic structure theory. *Int. Rev. Phys. Chem.* **2006**, *25*, 427–468.

(25) Kong, L.; Bischoff, F. A.; Valeev, E. F. Explicitly Correlated R12/F12 Methods for Electronic Structure. *Chem. Rev.* **2012**, *112*, 75–107.

(26) Ten-no, S. Initiation of explicitly correlated Slater-type geminal theory. *Chem. Phys. Lett.* **2004**, *398*, 56–61.

(27) Becke, A. D. Density-functional thermochemistry. III. The role of exact exchange. *J. Chem. Phys.* **1993**, *98*, 5648–5652.

(28) Stephens, P. J.; Devlin, F. J.; Chabalowski, C. F.; Fukuda, R. Ab Initio Calculation of Vibrational Absorption and Circular Dichroism Spectra Using Density Functional Force Fields. *J. Phys. Chem.* **1994**, *98*, 11623–11627.

(29) Perdew, J. P.; Ernzerhof, M.; Burke, K. Rationale for mixing exact exchange with density functional approximations. *J. Chem. Phys.* **1996**, *105*, 9982–9985.

(30) The DSD-BLYP functional has been optimized multiple times, here we refer to the frozen-core version with no dispersion correction optimized in Ref. 32, contains a fraction of 0.75 exact exchange. The D3BJ optimized functional contains a fraction of approximately 0.71 exact exchange. The XYG3 functional contains 0.8033 exact exchange.

(31) Kozuch, S.; Gruzman, D.; Martin, J. M. L. DSD-BLYP: A General Purpose Double Hybrid Density Functional Including Spin Component Scaling and Dispersion Correction. *J. Phys. Chem. C* **2010**, *114*, 20801–20808.

(32) Kozuch, S.; Martin, J. M. L. Spin-component-scaled double hybrids: An extensive

search for the best fifth-rung functionals blending DFT and perturbation theory. *J. Comput. Chem.* **2013**, *34*, 2327– 2344.

(33) Becke, A. D. Density-functional exchange-energy approximation with correct asymptotic behavior. *Phys. Rev. A* **1988**, *38*, 3098–3100.

(34) Lee, C.; Yang, W.; Parr, R. G. Development of the Colle-Salvetti correlation-energy formula into a functional of the electron density. *Phys. Rev. B* **1988**, *37*, 785–789.

(35) Martin, J. M. L.; Santra, G. Empirical Double-Hybrid Density Functional Theory: A 'Third Way' in Between WFT and DFT. *Isr. J. Chem.* **2020**, *60*, 1–19.

(36) Mardirossian, N.; Head-Gordon, M. Survival of the most transferable at the top of Jacob's ladder: Defining and testing the ω B97M(2) double hybrid density functional. *J. Chem. Phys.* **2018**, *148*, 241736.

(37) Becke, A. D. Density-functional thermochemistry. V. Systematic optimization of exchange-correlation functionals. *J. Chem. Phys.* **1997**, *107*, 8554–8560.

(38) Hamprecht, F. A.; Cohen, A. J.; Tozer, D. J.; Handy, N. C. Development and assessment of new exchange-correlation functionals. *J. Chem. Phys.* **1998**, *109*, 6264–6271.

(39) Grimme, S. Improved second-order Møller–Plesset perturbation theory by separate scaling of parallel- and antiparallel-spin pair correlation energies. *J. Chem. Phys.* **2003**, *118*, 9095–9102.

(40) Grimme, S.; Goerigk, L.; Fink, R. F. Spin-component-scaled electron correlation methods. *Wiley Interdiscip. Rev.: Comput. Mol. Sci.* **2012**, *2*, 886–906.

(41) Kozuch, S.; Martin, J. M. L. DSD-PBEP86: in search of the best double-hybrid DFT with spin-component scaled MP2 and dispersion corrections. *Phys. Chem. Chem. Phys.* **2011**, *13*, 20104–20107.

(42) Jung, Y.; Lochan, R. C.; Dutoi, A. D.; Head-Gordon, M. Scaled opposite-spin second order Møller–Plesset correlation energy: An economical electronic structure method. *J. Chem. Phys.* **2004**, *121*, 9793–9802.

(43) Goerigk, L.; Grimme, S. Efficient and Accurate Double-Hybrid-Meta-GGA Density Functionals—Evaluation with the Extended GMTKN30 Database for General Main Group Thermochemistry, Kinetics, and Noncovalent Interactions. *J. Chem. Theory Comput.* **2011**, *7*, 291–309.

(44) Zhang, I. Y.; Xu, X.; Jung, Y.; Goddard, W. A. A fast doubly hybrid density functional method close to chemical accuracy using a local opposite spin ansatz. *Proc. Natl. Acad. Sci. U. S. A.* **2011**, *108*, 19896–19900.

(45) Benighaus, T.; DiStasio, R. A.; Lochan, R. C.; Chai, J.-D.; Head-Gordon, M. Semiempirical Double-Hybrid Density Functional with Improved Description of Long-Range Correlation. *J. Phys. Chem. A* **2008**, *112*, 2702–2712.

(46) Chen, G. P.; Voora, V. K.; Agee, M. M.; Balasubramani, S. G.; Furche, F. Random-Phase Approximation Methods. *Annu. Rev. Phys. Chem.* **2017**, *68*, 421–445.

(47) Grimme, S. Density functional theory with London dispersion corrections. *Wiley Interdiscip. Rev.: Comput. Mol. Sci.* **2011**, *1*, 211–228.

(48) Klimeš, J.; Michaelides, A. Perspective: Advances and challenges in treating van der Waals dispersion forces in density functional theory. *J. Chem. Phys.* **2012**, *137*, 120901.

(49) Roch, L. M.; Baldridge, K. K. Dispersion-Corrected Spin-Component-Scaled Double-Hybrid Density Functional Theory: Implementation and Performance for Non-covalent Interactions. *J. Chem. Theory Comput.* **2017**, *13*, 2650–2666.

(50) Becke, A. D.; Johnson, E. R. A density-functional model of the dispersion interaction. *J. Chem. Phys.* **2005**, *123*, 154101.

(51) Johnson, E. R.; Becke, A. D. A post-Hartree–Fock model of intermolecular interactions. *J. Chem. Phys.* **2005**, *123*, 024101.

(52) Grimme, S.; Ehrlich, S.; Goerigk, L. Effect of the damping function in dispersion corrected density functional theory. *J. Comput. Chem.* **2011**, *32*, 1456–1465.

(53) Caldeweyher, E.; Bannwarth, C.; Grimme, S. Extension of the D3 dispersion coefficient model. *J. Chem. Phys.* **2017**, *147*, 034112.

(54) However, we do not utilise this method here. Instead we note that the dispersion could be re-optimised with this method in future.

(55) Eisenschitz, R.; London, F. Über das Verhältnis der van der Waalsschen Kräfte zu den homöopolaren Bindungskräften. *Z. Phys.* **1930**, *60*, 491–527.

(56) London, F. Zur Theorie und Systematik der Molekularkräfte. *Z. Phys.* **1930**, *63*, 245–279.

(57) London, F. The general theory of molecular forces. *Trans. Faraday Soc.* **1937**, *33*, 8b.

(58) For this work, note that B3LYP refers to the B3LYP5 version of B3LYP containing the VWN(V) correlation functional rather than the often used B3LYP3 including VWN(III) correlation.

(59) Goerigk, L.; Grimme, S. Double-hybrid density functionals. *Wiley Interdiscip. Rev.: Comput. Mol. Sci.* **2014**, *4*, 576–600.

(60) Goerigk, L.; Hansen, A.; Bauer, C.; Ehrlich, S.; Najibi, A.; Grimme, S. GMTKN24, GMTKN30 and GMTKN55 Databases. 2017 (accessed January 24, 2020); `https://www.chemie.uni-bonn.de/pctc/mulliken-center/software/GMTKN`.

(61) Curtiss, L. A.; Raghavachari, K.; Redfern, P. C.; Pople, J. A. Assessment of Gaussian-2 and density functional theories for the computation of enthalpies of formation. *J. Chem. Phys.* **1997**, *106*, 1063–1079.

(62) Curtiss, L. A.; Redfern, P. C.; Raghavachari, K.; Pople, J. A. Assessment of Gaussian-2 and density functional theories for the computation of ionization potentials and electron affinities. *J. Chem. Phys.* **1998**, *109*, 42–55.

(63) G2/97 Neutral Test Set Geometries. (accessed March 20, 2019); `http://www.cse.anl.gov/OldCHMwebsiteContent/compmat/g2igeoma.htm`.

(64) MP2(full)/6-31G* geometries for the G2/97 test set were obtained from the Argonne National Laboratory Web site. The geometries used are included in the supporting information.

(65) Werner, H.-J.; Knowles, P. J.; Manby, F. R.; Black, J. A.; Doll, K.; Heßelmann, A.; Kats, D.; Köhn, A.; Korona, T.; Kreplin, D. A.; Ma, Q.; Miller, T. F.; Mitrushchenkov, A.; Peterson, K. A.; Polyak, I.; Rauhut, G.; Sibaev, M. The Molpro quantum chemistry package. *J. Chem. Phys.* **2020**, *152*, 144107.

(66) Werner, H.-J.; Knowles, P. J.; Knizia, G.; Manby, F. R.; Schütz, M. Molpro: a general-purpose quantum chemistry program package. *Wiley Interdiscip. Rev.: Comput. Mol. Sci.* **2012**, *2*, 242–253.

(67) Werner, H.-J.; Knowles, P. J.; Knizia, G.; Manby, F. R.; Schütz, M.; Celani, P.; Györffy, W.; Kats, D.; Korona, T.; Lindh, R.; Mitrushenkov, A.; Rauhut, G.; Shamasundar, K. R.; Adler, T. B.; Amos, R. D.; Bennie, S. J.; Bernhardsson, A.; Berning, A.; Cooper, D. L.; Deegan, M. J. O.; Dobbyn, A. J.; Eckert, F.; Goll, E.; Hampel, C.; Hesselmann, A.; Hetzer, G.; Hrenar, T.; Jansen, G.; Köppl, C.; Lee, S. J. R.; Liu, Y.; Lloyd, A. W.; Ma, Q.; Mata, R. A.; May, A. J.; McNicholas, S. J.; Meyer, W.; Miller III, T. F.; Mura, M. E.; Nicklass, A.; O'Neill, D. P.; Palmieri, P.; Peng, D.; Pflüger, K.;

Pitzer, R.; Reiher, M.; Shiozaki, T.; Stoll, H.; Stone, A. J.; Tarroni, R.; Thorsteinsson, T.; Wang, M.; Welborn, M. MOLPRO, version 2019.2, a package of ab initio programs. 2019.

(68) Knowles, P. J.; Andrews, J. S.; Amos, R. D.; Handy, N. C.; Pople, J. A. Restricted Møller–Plesset Theory for Open Shell Molecules. *Chem. Phys. Lett.* **1991**, *186*, 130–136.

(69) Parrish, R. M.; Burns, L. A.; Smith, D. G. A.; Simmonett, A. C.; DePrince, A. E.; Hohenstein, E. G.; Bozkaya, U.; Sokolov, A. Y.; Di Remigio, R.; Richard, R. M.; Gonthier, J. F.; James, A. M.; McAlexander, H. R.; Kumar, A.; Saitow, M.; Wang, X.; Pritchard, B. P.; Verma, P.; Schaefer, H. F.; Patkowski, K.; King, R. A.; Valeev, E. F.; Evangelista, F. A.; Turney, J. M.; Crawford, T. D.; Sherrill, C. D. Psi4 1.1: An Open-Source Electronic Structure Program Emphasizing Automation, Advanced Libraries, and Interoperability. *J. Chem. Theory Comput.* **2017**, *13*, 3185–3197.

(70) DePrince, A. E.; Sherrill, C. D. Accuracy and Efficiency of Coupled-Cluster Theory Using Density Fitting/Cholesky Decomposition, Frozen Natural Orbitals, and a t_1-Transformed Hamiltonian. *J. Chem. Theory Comput.* **2013**, *9*, 2687–2696.

(71) Sun, Q.; Berkelbach, T. C.; Blunt, N. S.; Booth, G. H.; Guo, S.; Li, Z.; Liu, J.; McClain, J. D.; Sayfutyarova, E. R.; Sharma, S.; Wouters, S.; Chan, G. K. PySCF: the Python-based simulations of chemistry framework. 2017; `https://onlinelibrary.wiley.com/doi/abs/10.1002/wcms.1340`.

(72) Sun, Q. Libcint: An efficient general integral library for Gaussian basis functions. *J. Comput. Chem.* **2015**, *36*, 1664–1671.

(73) Manby, F. R.; Miller III, T. F.; Bygrave, P.; Ding, F.; Dresselhaus, T.; Batista-Romero, F.; Buccheri, A.; Bungey, C.; Lee, S.; Meli, R.; Miyamoto, K.; Stein-

mann, C.; Tsuchiya, T.; Welborn, M.; Wiles, T. C.; Williams, Z. 2019, DOI: 10.26434/chemrxiv.7762646.v2.

(74) Manby, F. R.; Miller III, T. F. Entos. 2019; https://www.entos.info.

(75) Dunning, T. H. Gaussian basis sets for use in correlated molecular calculations. I. The atoms boron through neon and hydrogen. *J. Chem. Phys.* **1989**, *90*, 1007–1023.

(76) Kendall, R. A.; Dunning, T. H.; Harrison, R. J. Electron affinities of the first-row atoms revisited. Systematic basis sets and wave functions. *J. Chem. Phys.* **1992**, *96*, 6796–6806.

(77) Woon, D. E.; Dunning, T. H. Gaussian basis sets for use in correlated molecular calculations. III. The atoms aluminum through argon. *J. Chem. Phys.* **1993**, *98*, 1358–1371.

(78) Woon, D. E.; Dunning, T. H. Gaussian basis sets for use in correlated molecular calculations. IV. Calculation of static electrical response properties. *J. Chem. Phys.* **1994**, *100*, 2975–2988.

(79) Dunning, T. H.; Peterson, K. A.; Wilson, A. K. Gaussian basis sets for use in correlated molecular calculations. X. The atoms aluminum through argon revisited. *J. Chem. Phys.* **2001**, *114*, 9244–9253.

(80) Curtiss, L. A.; Raghavachari, K.; Trucks, G. W.; Pople, J. A. Gaussian-2 theory for molecular energies of first- and second-row compounds. *J. Chem. Phys.* **1991**, *94*, 7221–7230.

(81) Lao, K. U.; Schäffer, R.; Jansen, G.; Herbert, J. M. Accurate Description of Intermolecular Interactions Involving Ions Using Symmetry-Adapted Perturbation Theory. *J. Chem. Theory Comput.* **2015**, *11*, 2473–2486.

(82) Weigend, F.; Furche, F.; Ahlrichs, R. Gaussian basis sets of quadruple zeta valence quality for atoms H–Kr. *J. Chem. Phys.* **2003**, *119*, 12753–12762.

(83) Weigend, F. Hartree–Fock exchange fitting basis sets for H to Rn. *J. Comput. Chem.* **2008**, *29*, 167–175.

(84) Hättig, C. Optimization of auxiliary basis sets for RI-MP2 and RI-CC2 calculations: Core–valence and quintuple-ζ basis sets for H to Ar and QZVPP basis sets for Li to Kr. *Phys. Chem. Chem. Phys.* **2005**, *7*, 59–66.

(85) These grids were used in both Entos Qcore and Molpro with index 4.

(86) Krack, M.; Köster, A. M. An adaptive numerical integrator for molecular integrals. *J. Chem. Phys.* **1998**, *108*, 3226–3234.

(87) Laqua, H.; Kussmann, J.; Ochsenfeld, C. An improved molecular partitioning scheme for numerical quadratures in density functional theory. *J. Chem. Phys.* **2018**, *149*, 204111.

(88) The DOD-BLYP functional from Ref. 32 was originally optimized to include a D3BJ dispersion term. Here we use this functional both with and without this term.

(89) The DSD-BLYP functional has been optimized multiple times, with the fraction of exact exchange dependent on both on whether frozen-core or all-electron MP2 correlation is used, and the type of dispersion correction included.[31,32] In this paper we use the frozen-core versions with no dispersion and with D3BJ from Ref. 32.

(90) The XYGJ-OS functional of Ref. 44 uses opposite spin only MP2 correlation. The original functional also used a local approximation for the opposite spin correlation for even greater efficiency. Here we use the full osMP2 in the functional.

(91) Møller, C.; Plesset, M. S. Note on an Approximation Treatment for Many-Electron Systems. *Phys. Rev.* **1934**, *46*, 618–622.

(92) The complete list of exponents, as well as the coefficients used in this paper are given in the supporting information.

(93) Zhao, Y.; Lynch, B. J.; Truhlar, D. G. Development and Assessment of a New Hybrid Density Functional Model for Thermochemical Kinetics. *J. Phys. Chem. A* **2004**, *108*, 2715–2719.

(94) Zhao, Y.; González-García, N.; Truhlar, D. G. Benchmark Database of Barrier Heights for Heavy Atom Transfer, Nucleophilic Substitution, Association, and Unimolecular Reactions and Its Use to Test Theoretical Methods. *J. Phys. Chem. A* **2005**, *109*, 2012–2018.

(95) Guner, V.; Khuong, K. S.; Leach, A. G.; Lee, P. S.; Bartberger, M. D.; Houk, K. N. A Standard Set of Pericyclic Reactions of Hydrocarbons for the Benchmarking of Computational Methods: The Performance of ab Initio, Density Functional, CASSCF, CASPT2, and CBS-QB3 Methods for the Prediction of Activation Barriers, Reaction Energetics, and Transition State Geometries. *J. Phys. Chem. A* **2003**, *107*, 11445–11459.

(96) Ess, D. H.; Houk, K. N. Activation Energies of Pericyclic Reactions: Performance of DFT, MP2, and CBS-QB3 Methods for the Prediction of Activation Barriers and Reaction Energetics of 1,3-Dipolar Cycloadditions, and Revised Activation Enthalpies for a Standard Set of Hydrocarbon. *J. Phys. Chem. A* **2005**, *109*, 9542–9553.

(97) Grimme, S.; Mück-Lichtenfeld, C.; Würthwein, E.-U.; Ehlers, A. W.; Goumans, T. P. M.; Lammertsma, K. Consistent Theoretical Description of 1,3-Dipolar Cycloaddition Reactions. *J. Phys. Chem. A* **2006**, *110*, 2583–2586.

(98) Dinadayalane, T. C.; Vijaya, R.; Smitha, A.; Sastry, G. N. Diels-Alder Reactivity of Butadiene and Cyclic Five-Membered Dienes ((CH) 4 X, X = CH 2 , SiH 2 , O,

NH, PH, and S) with Ethylene: A Benchmark Study. *J. Phys. Chem. A* **2002**, *106*, 1627–1633.

(99) Karton, A.; O'Reilly, R. J.; Chan, B.; Radom, L. Determination of barrier heights for proton exchange in small water, ammonia, and hydrogen fluoride clusters with G4(MP2)-type, MPn, and SCS-MPn procedures-a caveat. *J. Chem. Theory Comput.* **2012**, *8*, 3128–3136.

(100) Karton, A.; O'Reilly, R. J.; Radom, L. Assessment of theoretical procedures for calculating barrier heights for a diverse set of water-catalyzed proton-transfer reactions. *J. Phys. Chem. A* **2012**, *116*, 4211–4221.

(101) Zheng, J.; Zhao, Y.; Truhlar, D. G. The DBH24/08 Database and Its Use to Assess Electronic Structure Model Chemistries for Chemical Reaction Barrier Heights. *J. Chem. Theory Comput.* **2009**, *5*, 808–821.

(102) Johnson, E. R.; Mori-Sánchez, P.; Cohen, A. J.; Yang, W. Delocalization errors in density functionals and implications for main-group thermochemistry. *J. Chem. Phys.* **2008**, *129*, 204112.

(103) Friedrich, J.; Hänchen, J. Incremental CCSD(T)(F12*)—MP2: A Black Box Method To Obtain Highly Accurate Reaction Energies. *J. Chem. Theory Comput.* **2013**, *9*, 5381–5394.

(104) Friedrich, J. Efficient Calculation of Accurate Reaction Energies—Assessment of Different Models in Electronic Structure Theory. *J. Chem. Theory Comput.* **2015**, *11*, 3596–3609.

(105) Grimme, S.; Antony, J.; Ehrlich, S.; Krieg, H. A consistent and accurate ab initio parametrization of density functional dispersion correction (DFT-D) for the 94 elements H-Pu. *J. Chem. Phys.* **2010**, *132*, 154104.

(106) Goerigk, L.; Grimme, S. A General Database for Main Group Thermochemistry, Kinetics, and Noncovalent Interactions – Assessment of Common and Reparameterized (meta-)GGA Density Functionals. *J. Chem. Theory Comput.* **2009**, *6*, 107–126.

(107) Setiawan, D.; Kraka, E.; Cremer, D. Strength of the pnicogen bond in complexes involving group VA elements N, P, and AS. *J. Phys. Chem. A* **2015**, *119*, 1642–1656.

(108) Jurečka, P.; Šponer, J.; Černý, J.; Hobza, P. Benchmark database of accurate (MP2 and CCSD(T) complete basis set limit) interaction energies of small model complexes, DNA base pairs, and amino acid pairs. *Phys. Chem. Chem. Phys.* **2006**, *8*, 1985–1993.

(109) Řezáč, J.; Riley, K. E.; Hobza, P. S66: A Well-balanced Database of Benchmark Interaction Energies Relevant to Biomolecular Structures. *J. Chem. Theory Comput.* **2011**, *7*, 2427–2438.

(110) Gruzman, D.; Karton, A.; Martin, J. M. L. Performance of Ab Initio and Density Functional Methods for Conformational Equilibria of C n H 2 n +2 Alkane Isomers (n = 4-8). *J. Phys. Chem. A* **2009**, *113*, 11974–11983.

(111) Kesharwani, M. K.; Karton, A.; Martin, J. M. L. Benchmark ab Initio Conformational Energies for the Proteinogenic Amino Acids through Explicitly Correlated Methods. Assessment of Density Functional Methods. *J. Chem. Theory Comput.* **2016**, *12*, 444–454.

(112) Kozuch, S.; Bachrach, S. M.; Martin, J. M. Conformational Equilibria in Butane-1,4-diol: A Benchmark of a Prototypical System with Strong Intramolecular H-bonds. *J. Phys. Chem. A* **2014**, *118*, 293–303.

(113) Fogueri, U. R.; Kozuch, S.; Karton, A.; Martin, J. M. The Melatonin Conformer Space: Benchmark and Assessment of Wave Function and DFT Methods for a Paradigmatic Biological and Pharmacological Molecule. *J. Phys. Chem. A* **2013**, *117*, 2269–2277.

(114) Yu, L. J.; Karton, A. Assessment of theoretical procedures for a diverse set of isomerization reactions involving double-bond migration in conjugated dienes. *Chem. Phys.* **2014**, *441*, 166–177.

(115) Parthiban, S.; Martin, J. M. L. Assessment of W1 and W2 theories for the computation of electron affinities, ionization potentials, heats of formation, and proton affinities. *J. Chem. Phys.* **2001**, *114*, 6014–6029.

(116) Zhao, Y.; Truhlar, D. G. Assessment of Density Functionals for π Systems: Energy Differences between Cumulenes and Poly-ynes; Proton Affinities, Bond Length Alternation, and Torsional Potentials of Conjugated Polyenes; and Proton Affinities of Conjugated Shiff Bases. *J. Phys. Chem. A* **2006**, *110*, 10478–10486.

(117) Zhao, Y.; Ng, H. T.; Peverati, R.; Truhlar, D. G. Benchmark Database for Ylidic Bond Dissociation Energies and Its Use for Assessments of Electronic Structure Methods. *J. Chem. Theory Comput.* **2012**, *8*, 2824–2834.

(118) Korth, M.; Grimme, S. "Mindless" DFT Benchmarking. *J. Chem. Theory Comput.* **2009**, *5*, 993–1003.

(119) Karton, A.; Daon, S.; Martin, J. M. W4-11: A high-confidence benchmark dataset for computational thermochemistry derived from first-principles W4 data. *Chem. Phys. Lett.* **2011**, *510*, 165–178.

(120) Karton, A.; Tarnopolsky, A.; Lamère, J.-F.; Schatz, G. C.; Martin, J. M. L. Highly Accurate First-Principles Benchmark Data Sets for the Parametrization and Validation of Density Functional and Other Approximate Methods. Derivation of a Robust, Generally Applicable, Double-Hybrid Functional for Thermochemistry and Thermochemical Kinetics. *J. Phys. Chem. A* **2008**, *112*, 12868–12886.

(121) Yu, H.; Truhlar, D. G. Components of the Bond Energy in Polar Diatomic Molecules,

Radicals, and Ions Formed by Group-1 and Group-2 Metal Atoms. *J. Chem. Theory Comput.* **2015**, *11*, 2968–2983.

(122) Zhao, Y.; Tishchenko, O.; Gour, J. R.; Li, W.; Lutz, J. J.; Piecuch, P.; Truhlar, D. G. Thermochemical Kinetics for Multireference Systems: Addition Reactions of Ozone. *J. Phys. Chem. A* **2009**, *113*, 5786–5799.

(123) Janak, J. F. Proof that $\partial E/\partial n_i = \epsilon_i$ in density-functional theory. *Phys. Rev. B* **1978**, *18*, 7165–7168.

(124) Su, N. Q.; Yang, W.; Mori-Sánchez, P.; Xu, X. Fractional Charge Behavior and Band Gap Predictions with the XYG3 Type of Doubly Hybrid Density Functionals. *J. Phys. Chem. A* **2014**, *118*, 9201–9211.

(125) Mardirossian, N.; Head-Gordon, M. ωB97X-V: A 10-parameter, range-separated hybrid, generalized gradient approximation density functional with nonlocal correlation, designed by a survival-of-the-fittest strategy. *Phys. Chem. Chem. Phys.* **2014**, *16*, 9904.

(126) Santra, G.; Sylvetsky, N.; Martin, J. M. L. Minimally Empirical Double-Hybrid Functionals Trained against the GMTKN55 Database: revDSD-PBEP86-D4, revDOD-PBE-D4, and DOD-SCAN-D4. *J. Phys. Chem. A* **2019**, *123*, 5129–5143.

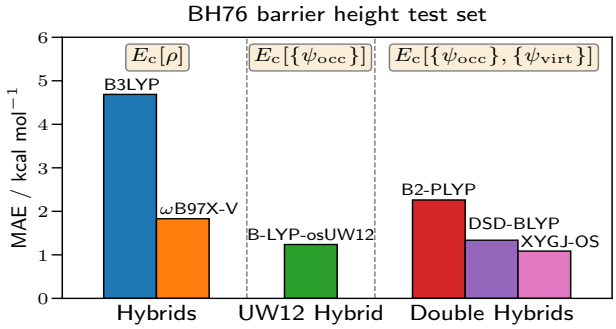

Figure 18: For Table of Contents Only